

Diluted Magnetic Semiconductors

- An Introduction -

Hideo Ohno^{1,2}



CSIS



¹Center for Spintronics Integrated Systems, Tohoku University, Sendai, Japan

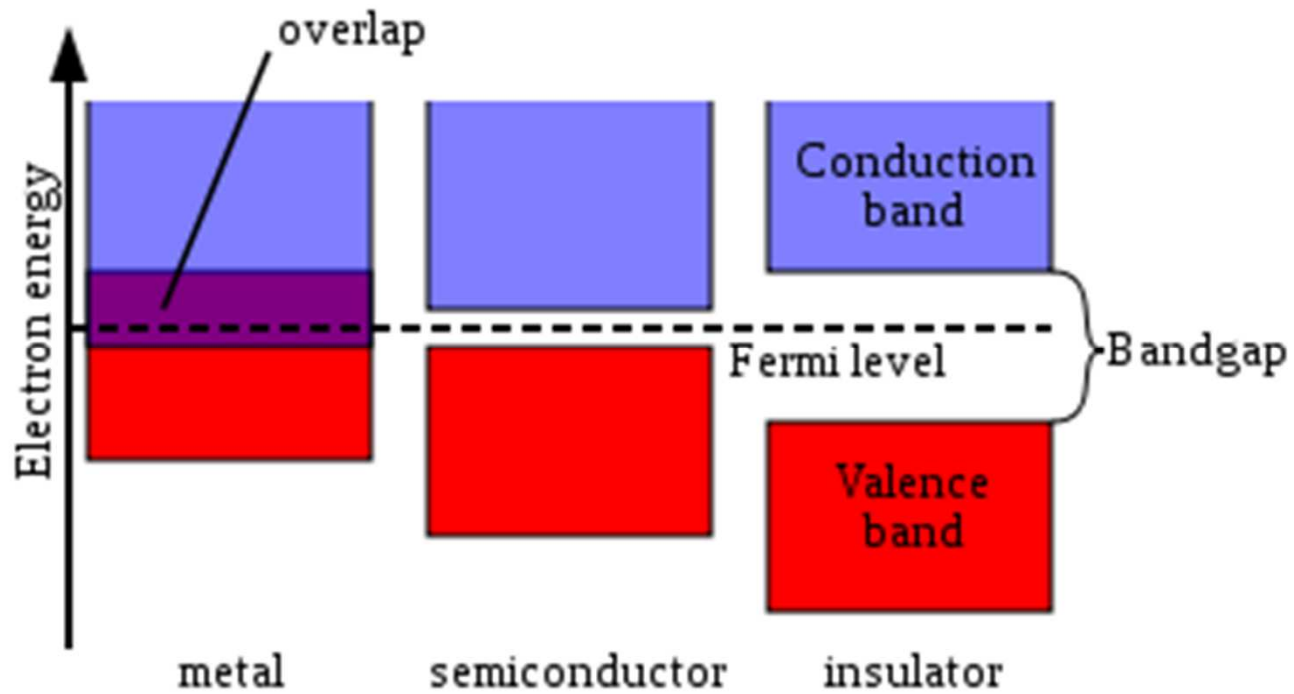
²Laboratory for Nanoelectronics and Spintronics, Research Institute of Electrical Communication, Tohoku University, Sendai, Japan

1. What you need to know about nonmagnetic semiconductors
 - Band structure
2. How you make a semiconductor magnetic
 - Doping and *sp-d* exchange
3. The consequences of exchange interaction
 - Spin-split bands and ferromagnetism
4. Making "use" of ferromagnetism in semiconductors
 - Electrical control of ferromagnetism
 - Current induced domain wall motion
 - Tunneling with magnetism

I am indebted to lecturers of earlier Spintechs, many collaborators, particularly Tomasz Dietl and Fumihiro Matsukura, for a number of materials used here.

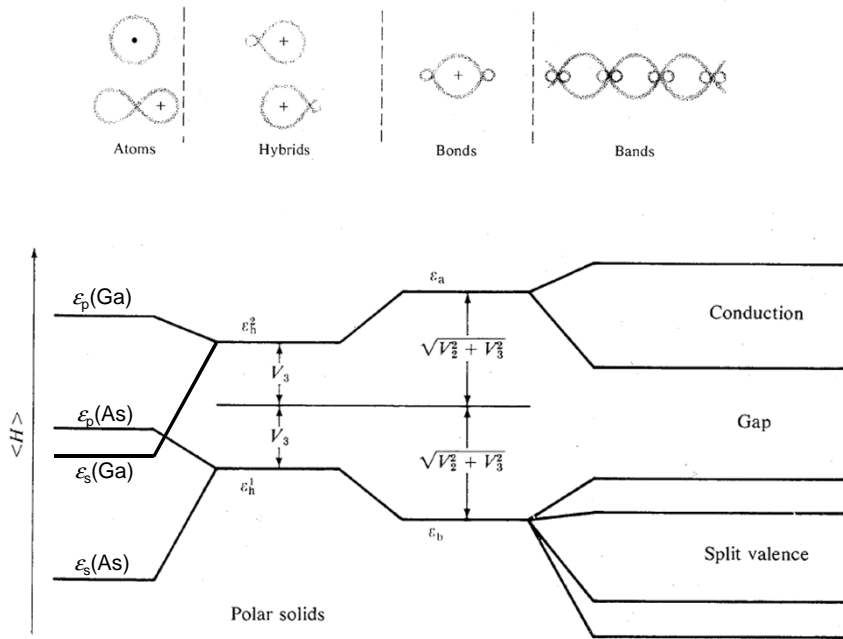
1. What you need to know about nonmagnetic semiconductors

- **Band structure**

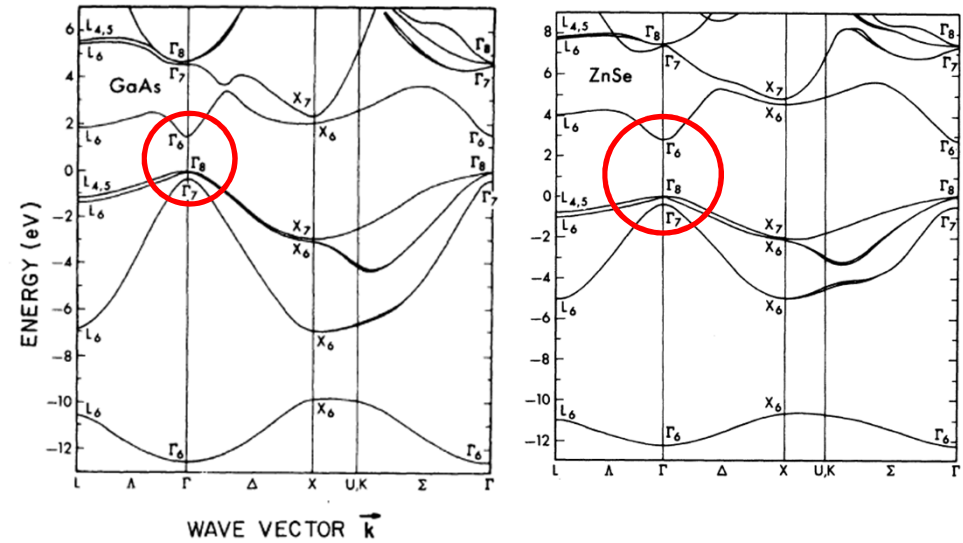


Electronic band structure

From Wikipedia, the free encyclopedia

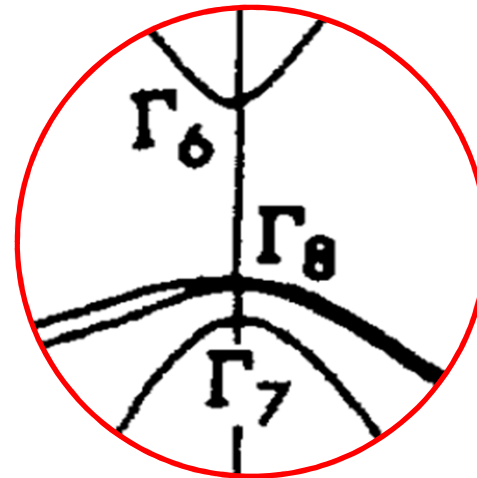


taken from Walter A. Harrison "Electronic Structure and the Properties of Solids -The Physics of Chemical Bond -, 1980

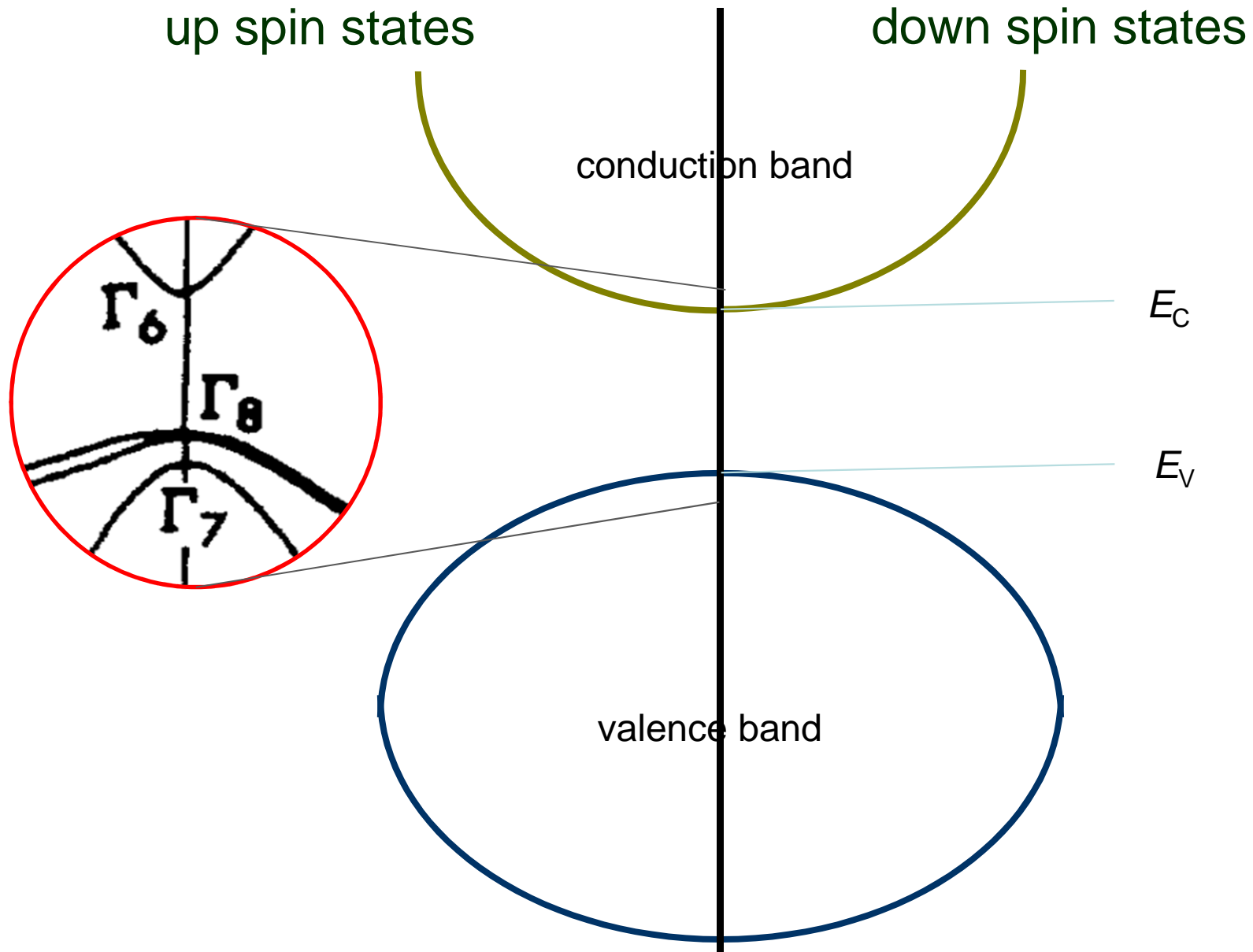


J. R. Chelikowsky and M. L. Cohen, *Phys. Rev.* **B14**, 556 (1976)

Bottom of the conduction band: **Ga 4s**
 Top of the valence band: **As 4p**



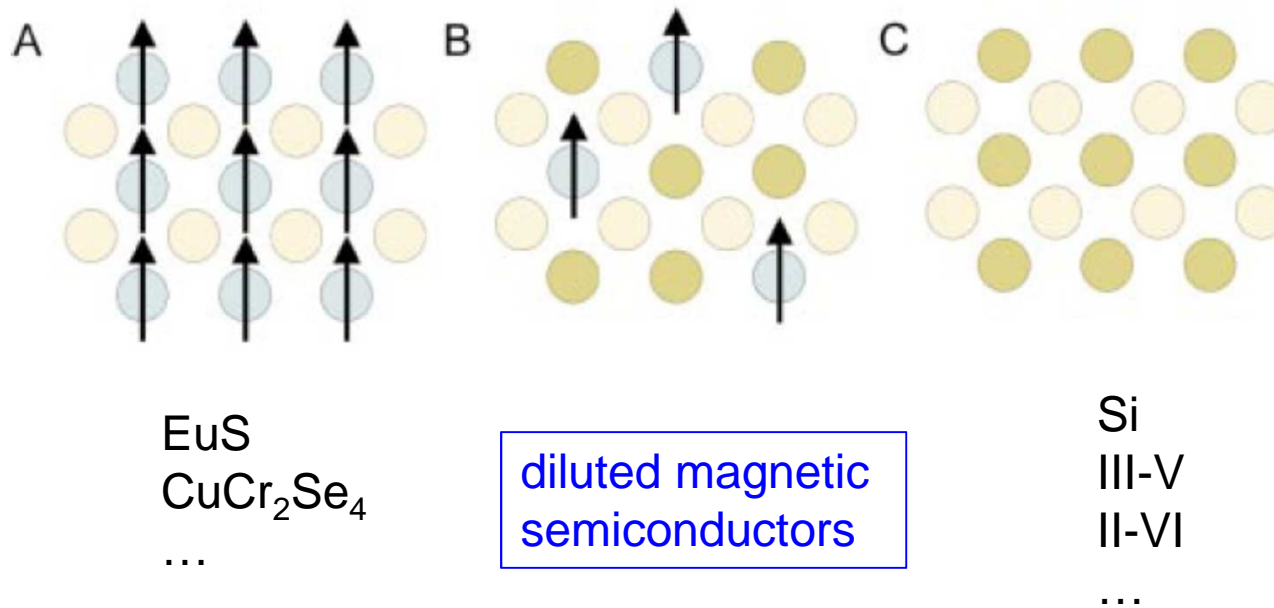
Density of states



2. How you make a semiconductor magnetic

- Doping and *sp-d* exchange

Making semiconductor magnetic



Magnetic ion: Mn

PERIODIC TABLE
Atomic Properties of the Elements

NIST
National Institute of Standards and Technology
Technology Administration, U.S. Department of Commerce

Frequently used fundamental physical constants
For the most accurate values of these and other constants, visit physics.nist.gov/constants
1 second = 9 192 631 770 periods of radiation corresponding to the transition between the two hyperfine levels of the ground state of ¹³³Cs

speed of light in vacuum c 299 792 458 m s⁻¹ (exact)
Planck constant h 6.626 070 15 × 10⁻³⁴ J s ($\hbar = h/2\pi$)
elementary charge e 1.602 176 634 × 10⁻¹⁹ C
electron mass m_e 9.109 383 56 × 10⁻³¹ kg
 $m_e c^2$ 0.5110 MeV
proton mass m_p 1.672 621 7 × 10⁻²⁷ kg
fine-structure constant α 1/137.035 999 074
Rydberg constant R_∞ 10 973 731.762 53 m⁻¹
 $R_\infty hc$ 13.605 698 06 eV
Boltzmann constant k 1.380 658 × 10⁻²³ J K⁻¹

Solids
 Liquids
 Gases
 Artificially Prepared

Physics Laboratory
 physics.nist.gov
 Standard Reference Data Group
 www.nist.gov/srd

Group	1	2	3	4	5	6	7	8	9	10	11	12	13	14	15	16	17	18
IA	IIA	IIIB	IVB	VB	VIB	VII	VIII	VIII	VIII	IB	IIB	IIIA	IVA	VA	VIA	VIIA	VIIIA	
1	H Hydrogen 1.00794 1s																	He Helium 4.002602 1s ²
2	Li Lithium 6.941 1s ² 2s	Be Beryllium 9.012182 1s ² 2s ²											B Boron 10.811 1s ² 2s ² 2p	C Carbon 12.0107 1s ² 2s ² 2p ²	N Nitrogen 14.0067 1s ² 2s ² 2p ³	O Oxygen 15.9994 1s ² 2s ² 2p ⁴	F Fluorine 18.9984032 1s ² 2s ² 2p ⁵	Ne Neon 20.1797 1s ² 2s ² 2p ⁶
3	Na Sodium 22.989770 [Ne]3s	Mg Magnesium 24.3050 [Ne]3s ²											Al Aluminum 26.981538 [Ne]3s ² 3p	Si Silicon 28.0855 [Ne]3s ² 3p ²	P Phosphorus 30.973761 [Ne]3s ² 3p ³	S Sulfur 32.065 [Ne]3s ² 3p ⁴	Cl Chlorine 35.453 [Ne]3s ² 3p ⁵	Ar Argon 39.948 [Ne]3s ² 3p ⁶
4	K Potassium 39.0983 [Ar]4s	Ca Calcium 40.078 [Ar]4s ²	Sc Scandium 44.955910 [Ar]3d ¹ 4s ²	Ti Titanium 47.867 [Ar]3d ² 4s ²	V Vanadium 50.9415 [Ar]3d ³ 4s ²	Cr Chromium 51.9961 [Ar]3d ⁵ 4s	Mn Manganese 54.938049 [Ar]3d ⁵ 4s ²	Fe Iron 55.845 [Ar]3d ⁶ 4s ²	Co Cobalt 58.933200 [Ar]3d ⁷ 4s ²	Ni Nickel 58.6934 [Ar]3d ⁸ 4s ²	Cu Copper 63.546 [Ar]3d ¹⁰ 4s	Zn Zinc 65.409 [Ar]3d ¹⁰ 4s ²	Ga Gallium 69.723 [Ar]3d ¹⁰ 4s ² 4p	Ge Germanium 72.64 [Ar]3d ¹⁰ 4s ² 4p ²	As Arsenic 74.92160 [Ar]3d ¹⁰ 4s ² 4p ³	Se Selenium 78.96 [Ar]3d ¹⁰ 4s ² 4p ⁴	Br Bromine 79.904 [Ar]3d ¹⁰ 4s ² 4p ⁵	Kr Krypton 83.798 [Ar]3d ¹⁰ 4s ² 4p ⁶
5	Rb Rubidium 85.4678 [Kr]5s	Sr Strontium 87.62 [Kr]5s ²	Y Yttrium 88.90585 [Kr]4d ¹ 5s ²	Zr Zirconium 91.224 [Kr]4d ² 5s ²	Nb Niobium 92.90638 [Kr]4d ⁴ 5s	Mo Molybdenum 95.94 [Kr]4d ⁵ 5s ¹	Tc Technetium (98) [Kr]4d ⁵ 5s ²	Ru Ruthenium 101.07 [Kr]4d ⁷ 5s ¹	Rh Rhodium 102.90550 [Kr]4d ⁸ 5s ¹	Pd Palladium 106.42 [Kr]4d ¹⁰	Ag Silver 107.8682 [Kr]4d ¹⁰ 5s ¹	Cd Cadmium 112.411 [Kr]4d ¹⁰ 5s ²	In Indium 114.818 [Kr]4d ¹⁰ 5s ² 5p	Sn Tin 118.710 [Kr]4d ¹⁰ 5s ² 5p ²	Sb Antimony 121.760 [Kr]4d ¹⁰ 5s ² 5p ³	Te Tellurium 127.60 [Kr]4d ¹⁰ 5s ² 5p ⁴	I Iodine 126.90447 [Kr]4d ¹⁰ 5s ² 5p ⁵	Xe Xenon 131.293 [Kr]4d ¹⁰ 5s ² 5p ⁶

<http://physics.nist.gov>

Hund rule: Distributing n electrons over $2(2l+1)$ degenerate atomic orbitals, the lowest energy state is the state that maximize the total spin angular momentum S

Mn: $l=2, n=5 \rightarrow S=5/2$

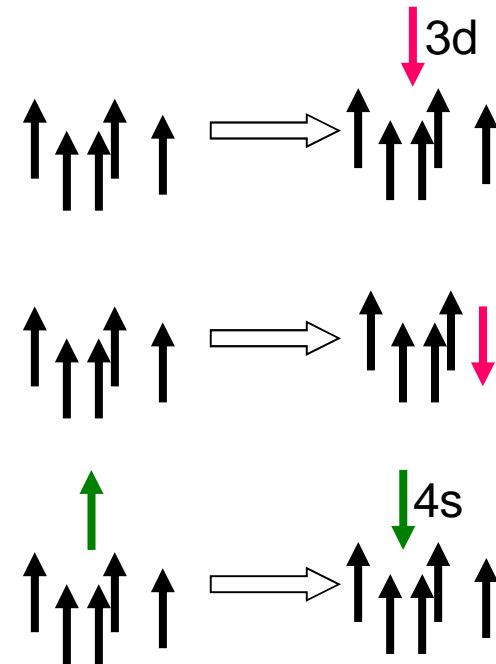
Magnetic ion: Mn

- intra site correlation energy $U = E_{n+1} - E_n$
for $n = 5$, $U \approx 15$ eV

- intra-site exchange interaction: *ferromagnetic*
Hund's rule: S the highest possible
for $n = 5$, $E_{S=3/2} - E_{S=5/2} \approx 2$ eV

- transition metal atoms, $3d^n 4s^1$, e.g., Mn: *ferromagnetic*

$$E_{S=2} - E_{S=3} \approx 1.2 \text{ eV} \rightarrow J_{s-d} \approx 0.4 \text{ eV}$$



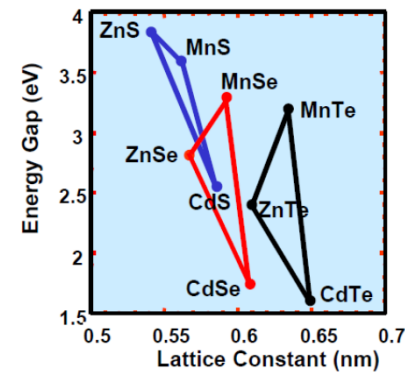
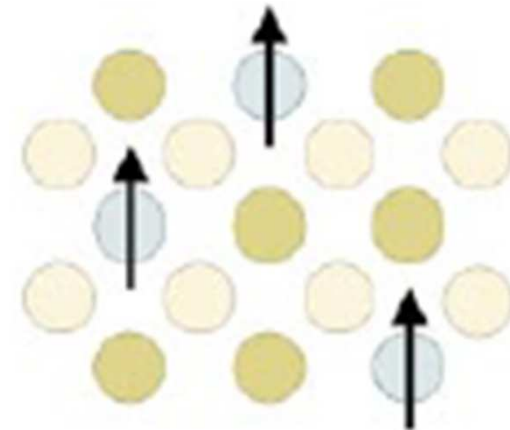
II-VI Diluted Magnetic Semiconductors

5 B Boron 10.811 $1s^2 2s^2 2p^1$ 8.2980	6 C Carbon 12.0107 $1s^2 2s^2 2p^2$ 11.2603	7 N Nitrogen 14.0064 $1s^2 2s^2 2p^3$ 14.5339	8 O Oxygen 15.9994 $1s^2 2s^2 2p^4$ 13.6181
13 Al Aluminum 26.981538 $[Ne]3s^2 3p^1$ 5.9858	14 Si Silicon 28.0855 $[Ne]3s^2 3p^2$ 8.1517	15 P Phosphorus 30.973761 $[Ne]3s^2 3p^3$ 10.4867	16 S Sulfur 32.065 $[Ne]3s^2 3p^4$ 10.3600
30 Zn Zinc 65.409 $[Ar]3d^{10} 4s^2$ 9.3942	31 Ga Gallium 69.723 $[Ar]3d^{10} 4s^2 4p^1$ 5.9993	32 Ge Germanium 72.64 $[Ar]3d^{10} 4s^2 4p^2$ 7.8994	33 As Arsenic 74.92160 $[Ar]3d^{10} 4s^2 4p^3$ 9.7883
48 Cd Cadmium 112.411 $[Kr]4d^{10} 5s^2$ 8.9938	49 In Indium 114.818 $[Kr]4d^{10} 5s^2 5p^1$ 5.7864	50 Sn Tin 118.710 $[Kr]4d^{10} 5s^2 5p^2$ 7.3439	51 Sb Antimony 121.760 $[Kr]4d^{10} 5s^2 5p^3$ 8.6084
80 Hg Mercury 200.59 $[Xe]4f^{14} 5d^{10} 6s^2$ 10.4375	81 Tl Thallium 204.3833 $[Hg]6p^1$ 6.1082	82 Pb Lead 207.2 $[Hg]6p^2$ 7.4167	83 Bi Bismuth 208.98038 $[Hg]6p^3$ 7.2855
			84 Po Polonium (209) $[Hg]6p^4$ 8.414

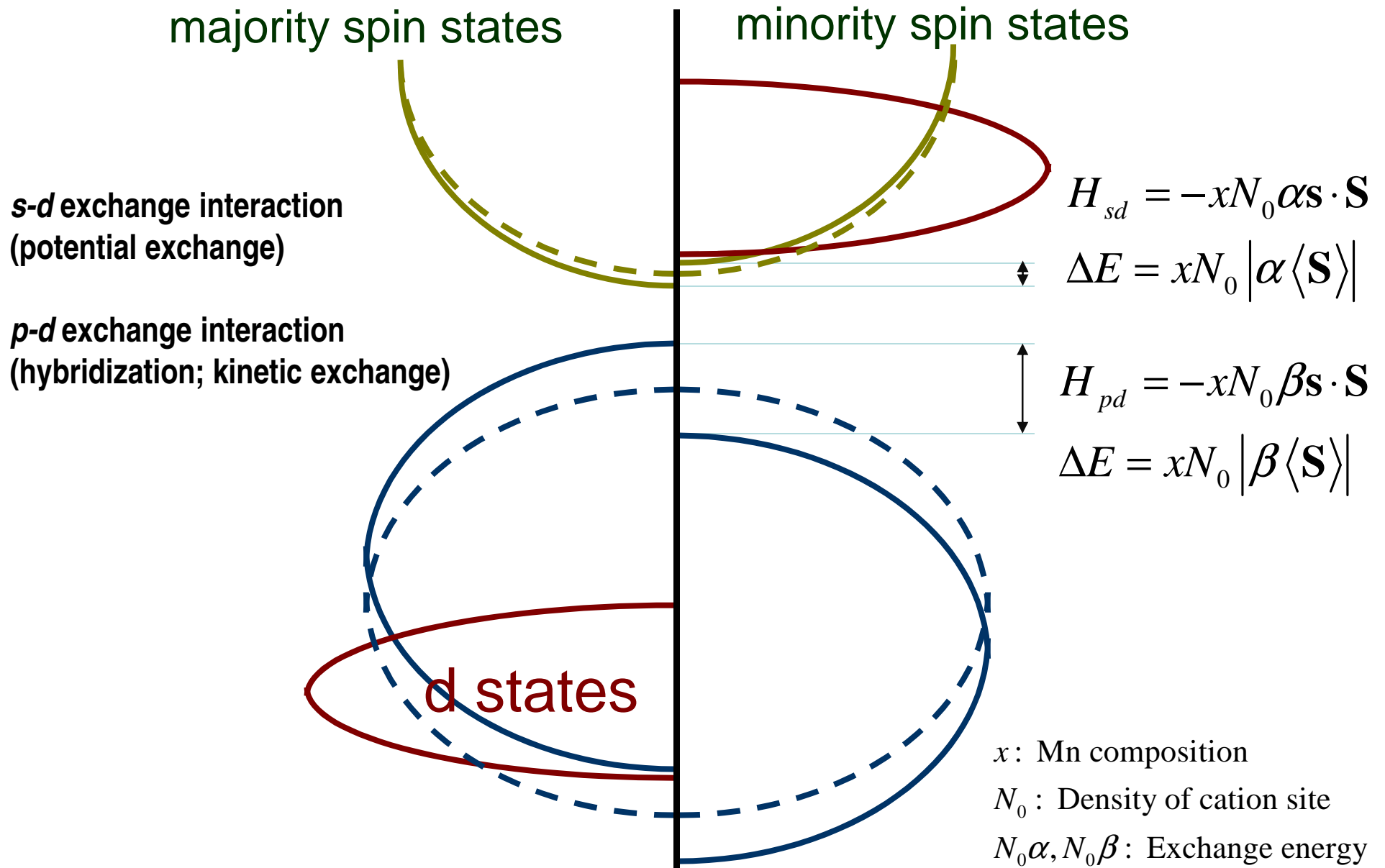
+

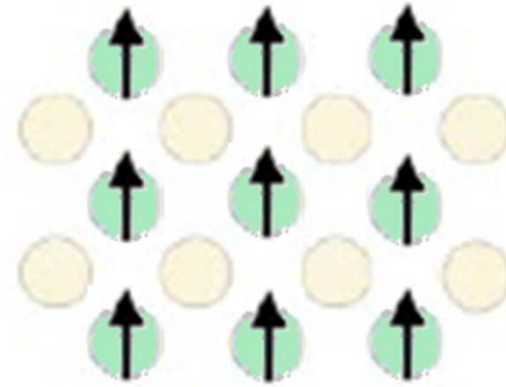
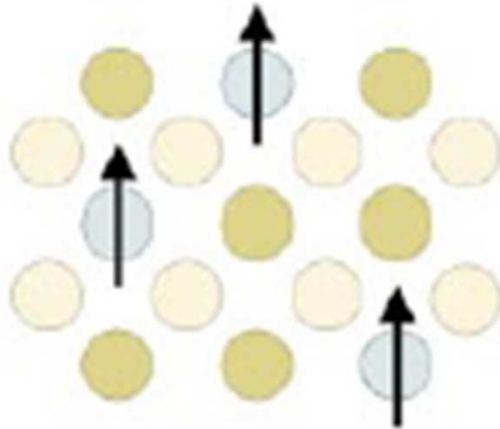
25 Mn Manganese 54.938049 $[Ar]3d^5 4s^2$ 7.4340
--

=



Density of states with transition metal impurity





Virtual crystal approximation

$$H_n = (1-x)U_0(\mathbf{r}-\mathbf{R}_n) + xU(\mathbf{r}-\mathbf{R}_n) - xJ(\mathbf{r}-\mathbf{R}_n)\mathbf{s}\cdot\mathbf{S}_n$$

molecular-field approximation

$$\frac{x}{V} \sum_n \mathbf{S}_n \rightarrow xN_0 \langle \mathbf{S}(\mathbf{r}) \rangle$$

$$\rightarrow -\frac{\mathbf{M}(\mathbf{r})}{g\mu_B}; \quad \mathbf{M}(\mathbf{r}) = -xN_0 g\mu_B \langle \mathbf{S}(\mathbf{r}) \rangle$$

mean-field approximation

$$\rightarrow -\frac{\mathbf{M}}{g\mu_B}; \quad \mathbf{M} = \langle \mathbf{M}(\mathbf{r}) \rangle$$

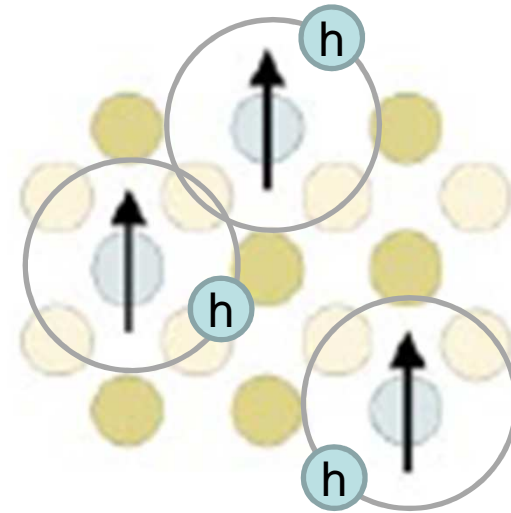
III-V Diluted Magnetic Semiconductors

5 $2p_{1/2}^0$		6 $3p_0$		7 $3p_{1/2}$		8 $3p_{3/2}$			
B Boron 10.811 $1s^2 2s^2 2p^1$ 8.263		C Carbon 12.0107 $1s^2 2s^2 2p^2$ 11.280		N Nitrogen 14.0067 $1s^2 2s^2 2p^3$ 14.5341		O Oxygen 15.9994 $1s^2 2s^2 2p^4$ 16.181			
13 $3p_{1/2}^0$		14 $3p_0$		15 $3p_{1/2}$		16 $3p_{3/2}$			
Al Aluminum 26.981538 $[\text{Ne}]3s^2 3p^1$ 5.9858		Si Silicon 28.0855 $[\text{Ne}]3s^2 3p^2$ 8.1117		P Phosphorus 30.973761 $[\text{Ne}]3s^2 3p^3$ 10.4867		S Sulfur 32.065 $[\text{Ne}]3s^2 3p^4$ 10.9900			
30 S_0		31 $2p_{1/2}^0$		32 $3p_0$		33 $4s_{3/2}^0$		34 $3p_{3/2}$	
Zn Zinc 65.409 $[\text{Ar}]3d^{10} 4s^2$ 9.3912		Ga Gallium 69.723 $[\text{Ar}]3d^{10} 4s^2 4p^1$ 5.9993		Ge Germanium 72.64 $[\text{Ar}]3d^{10} 4s^2 4p^2$ 7.814		As Arsenic 74.92160 $[\text{Ar}]3d^{10} 4s^2 4p^3$ 9.7886		Se Selenium 78.96 $[\text{Ar}]3d^{10} 4s^2 4p^4$ 9.724	
48 S_0		49 $2p_{1/2}^0$		50 $3p_0$		51 $4s_{3/2}^0$		52 $3p_{3/2}$	
Cd Cadmium 112.41 $[\text{Kr}]4d^{10} 5s^2$ 8.9938		In Indium 114.818 $[\text{Kr}]4d^{10} 5s^2 5p^1$ 5.7864		Sn Tin 118.71 $[\text{Kr}]4d^{10} 5s^2 5p^2$ 7.3436		Sb Antimony 121.760 $[\text{Kr}]4d^{10} 5s^2 5p^3$ 8.6084		Te Tellurium 127.60 $[\text{Kr}]4d^{10} 5s^2 5p^4$ 9.0096	
80 $1S_0$		81 $2p_{1/2}^0$		82 $3p_0$		83 $4s_{3/2}^0$		84 $3p_{3/2}$	
Hg Mercury 200.59 $[\text{Xe}]4f^{14} 5d^{10} 6s^2$ 10.4375		Tl Thallium 204.3833 $[\text{Hg}]6p^1$ 6.1082		Pb Lead 207.2 $[\text{Hg}]6p^2$ 7.4167		Bi Bismuth 208.98038 $[\text{Hg}]6p^3$ 7.2855		Po Polonium (209) $[\text{Hg}]6p^4$ 8.414	

+

25 $6s_{5/2}$
Mn
Manganese
54.938049
$[\text{Ar}]3d^5 4s^2$
7.4340

=



not to scale

(Ga,Mn)As, (In,Mn)As, (Ga,Mn)Sb

Mn in GaAs

Mn on Ga site: 113 meV acceptor

- **d⁵+hole (weak coupling)** ←
- d⁴
- d⁵+hole (strong coupling)

from spectroscopy

$$H = T - \frac{e^2}{\epsilon r} - V_0 \exp\left(-\left(\frac{r}{r_0}\right)^2\right) - xN_0\beta\mathbf{s} \cdot \mathbf{S} \quad N_0\beta = -0.9 \text{ eV}$$

kinetic, Coulomb, central cell correction, *p-d* exchange interaction

3. The consequences of exchange interaction

- **Spin-split bands** and ferromagnetism

Magnetization of localized spins – no holes

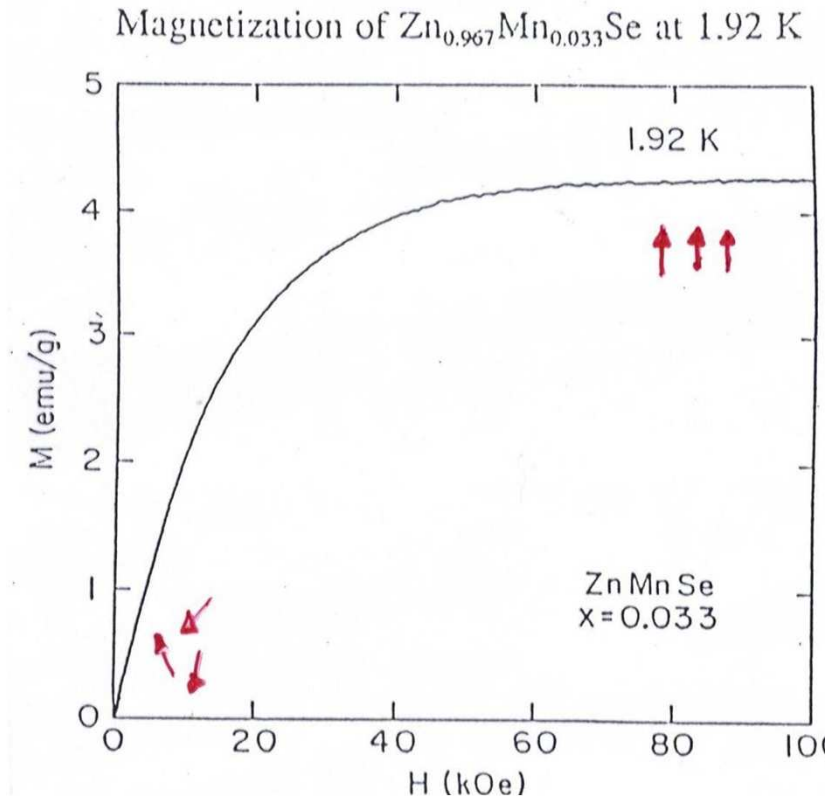
$$M(T,H) = g\mu_B S x_{eff} N_0 B_S [g\mu_B H / k_B (T + T_{AF})]$$

antiferromagnetic interactions

$$x_{eff} < x$$

$$T_{AF} > 0$$

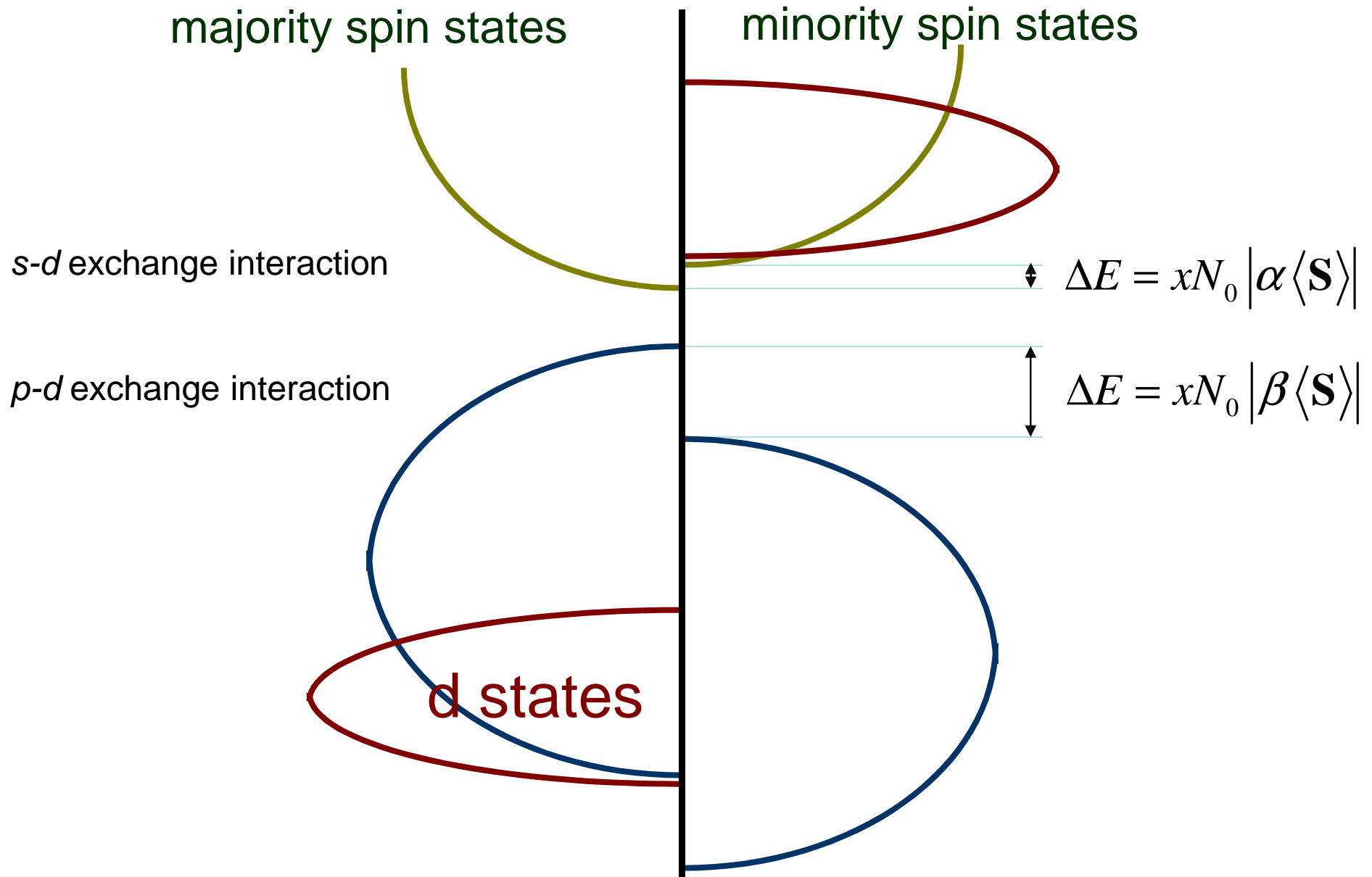
Modified Brillouin function



Y. Shapira et al.

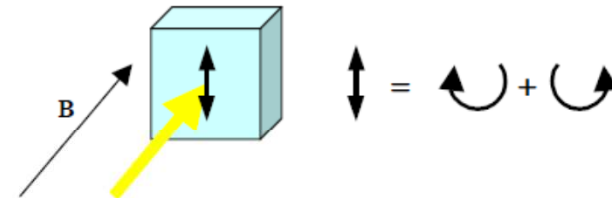
no spontaneous magnetization

Density of states with transition metal impurity



Faraday rotation

- A linearly polarized light arriving in the medium can be decomposed in two circularly polarized waves

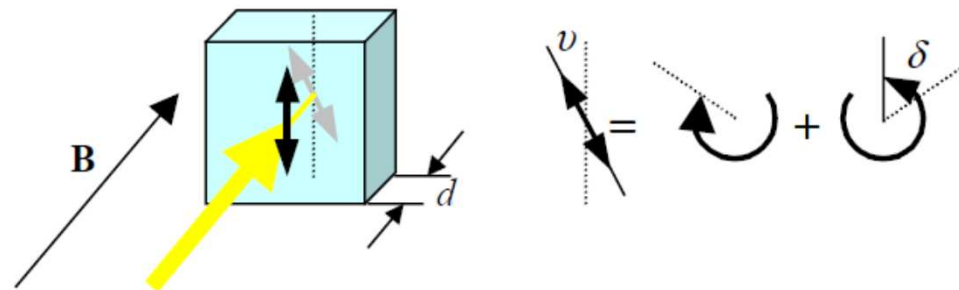


- After travelling in the medium over a distance d the two components develop a phase shift

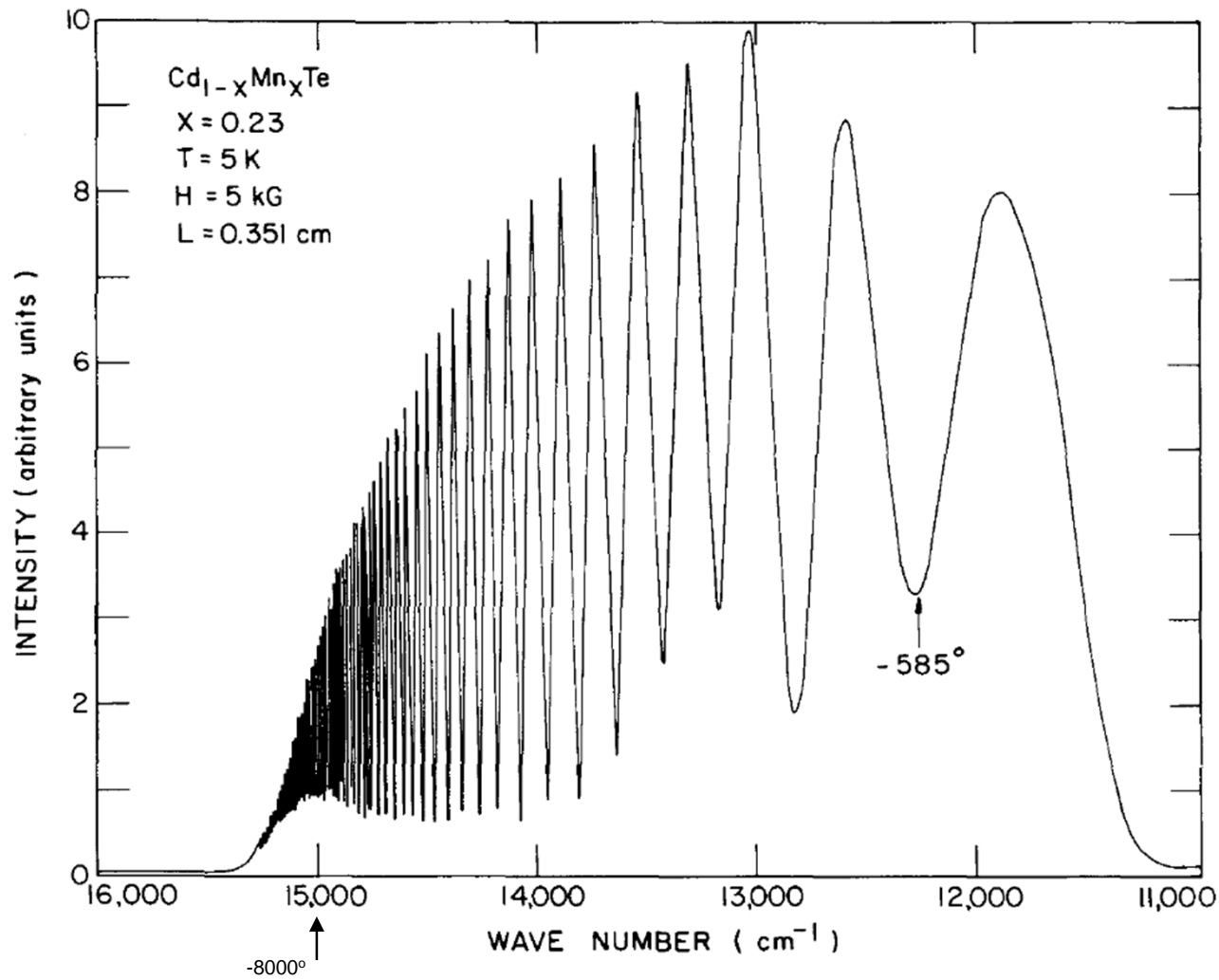
$$\delta = \frac{\omega}{c}(n_+ - n_-)d$$

- equivalent to a rotation of the polarization plane by the Faraday rotation angle

$$\vartheta = \frac{1}{2} \delta = \frac{\omega}{2c}(n_+ - n_-)d$$

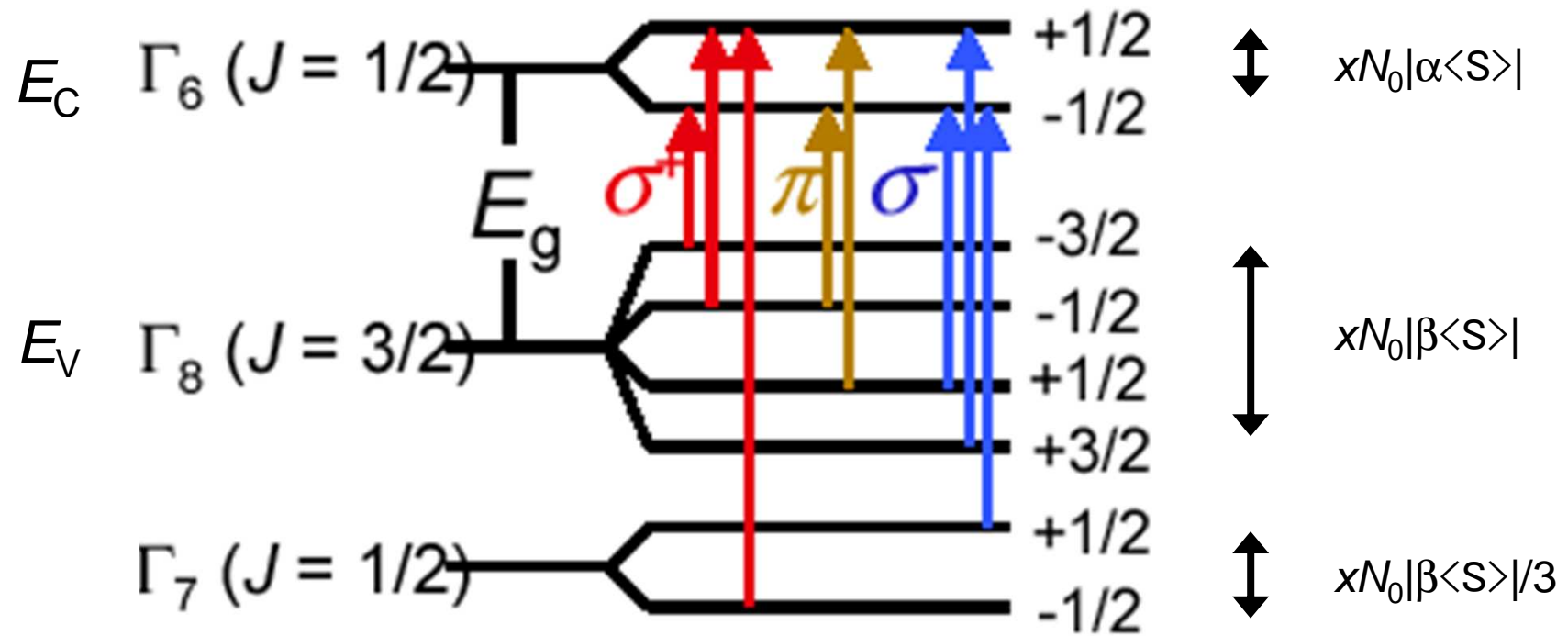


Faraday effect

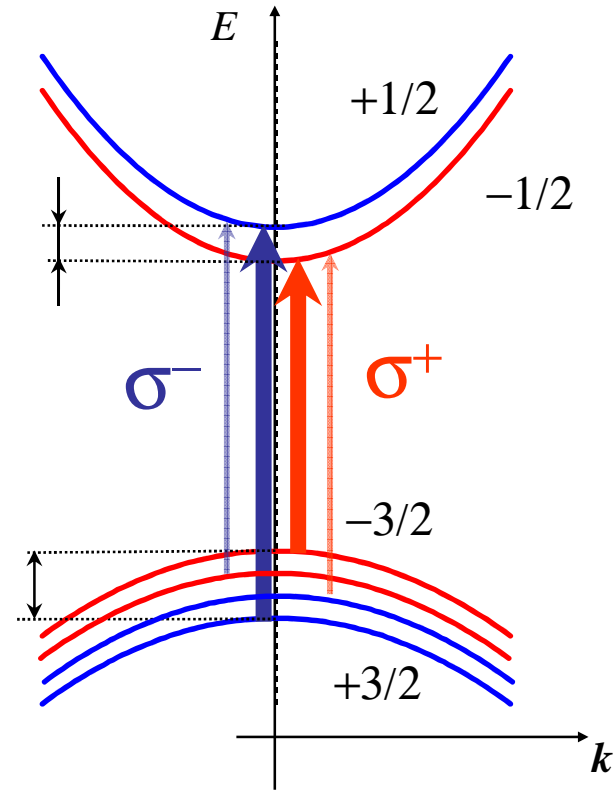
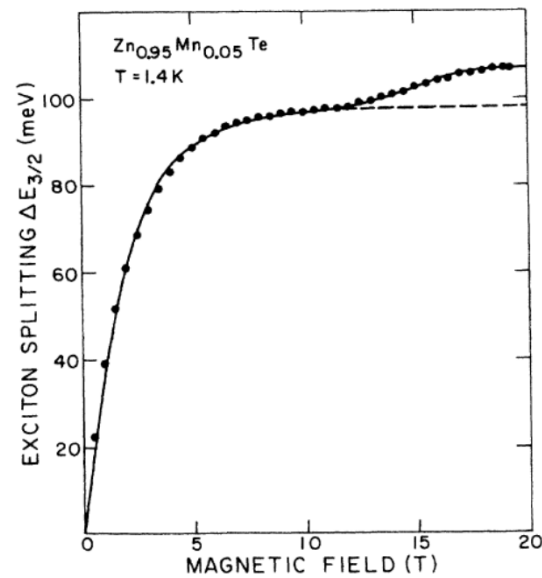
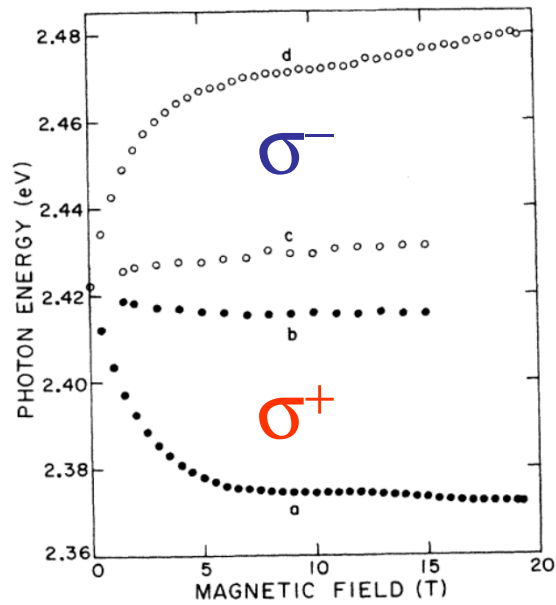


J. A. Gaj, R. R. Galazka, and M. Nawrocki, *Solid State Commun.*, vol. 25, p. 193 (1978).

Splitting of the bands



Measurements of the band splitting



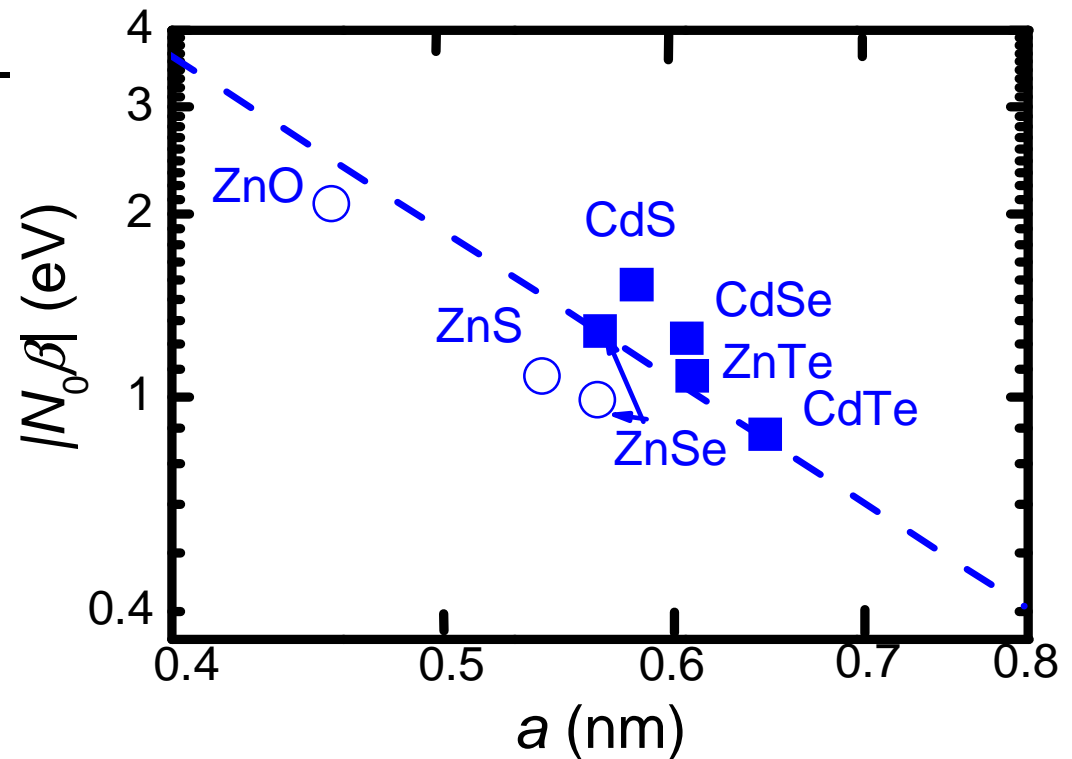
$$\Delta E = 2g_{\text{eff}}\mu_B HS, S=1/2$$

- $g_{\text{eff}} \sim 400 > 0$

- Follows M not H

sp-d exchange

material	$N_0\alpha$ (eV)	$N_0\beta$ (eV)
(Cd,Mn)Te	0.22	-0.88
(Cd,Mn)Se	0.26	-1.24
(Cd,Mn)S	0.22	-1.8
(Zn,Mn)Te	0.19	-1.09
(Zn,Mn)Se	0.26	-1.32
(Cd,Fe)Se	0.25	-1.45
(Zn,Fe)Se	0.22	-1.74
(Cd,Co)Se	0.28	-1.87



circles: photoemission
squares: optical spectroscopy

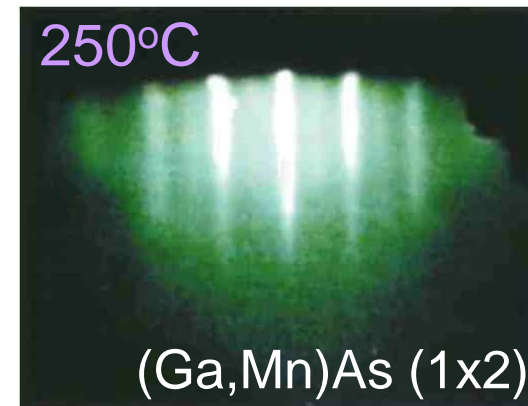
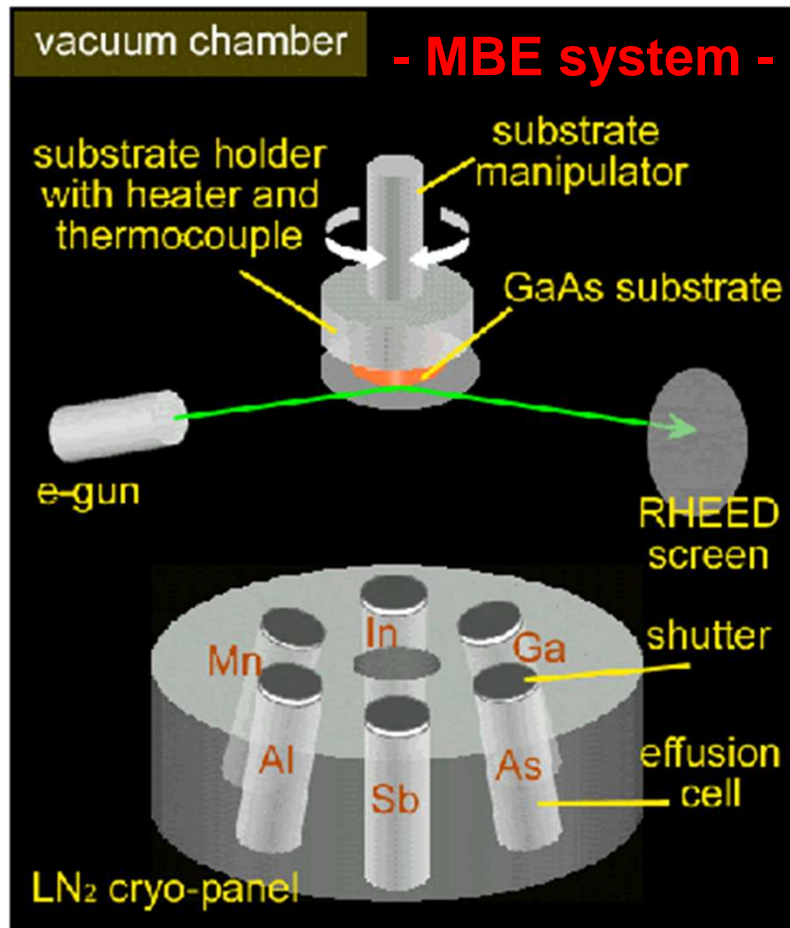
3. The consequences of exchange interaction

- Spin-split bands and ferromagnetism

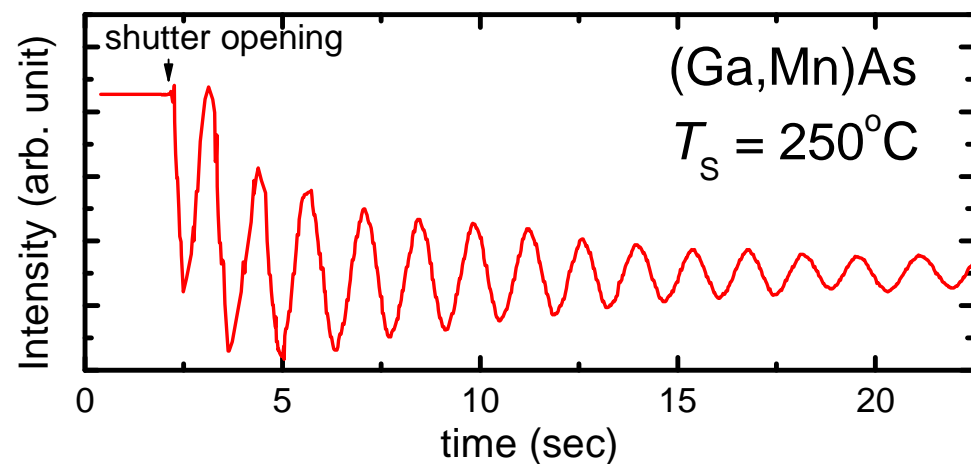
GaAs (or InAs) + Mn

Material Science

Molecular beam epitaxy of (Ga,Mn)As



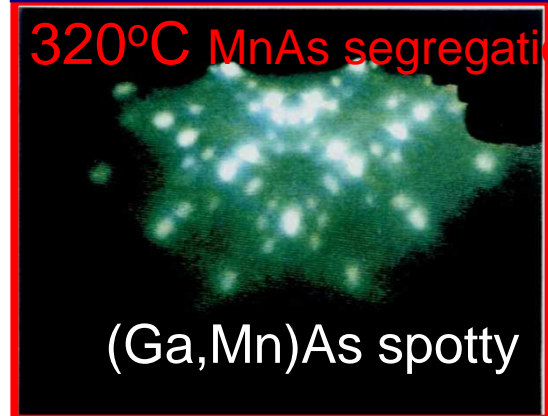
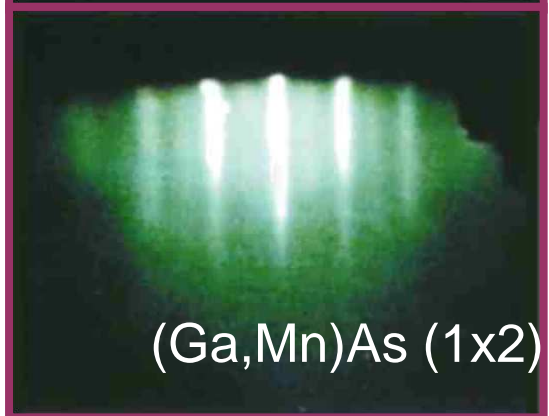
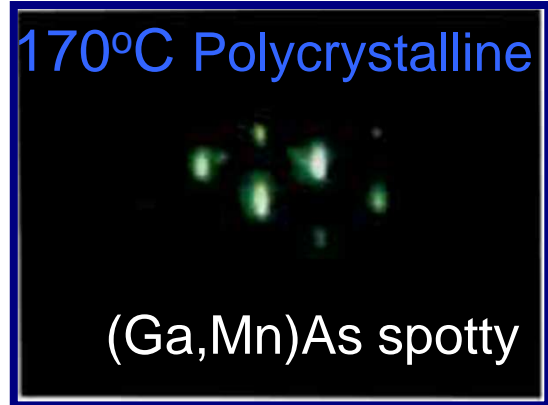
Single crystal (Ga,Mn)As



Molecular beam epitaxy of (Ga,Mn)As



[-110] azimuth

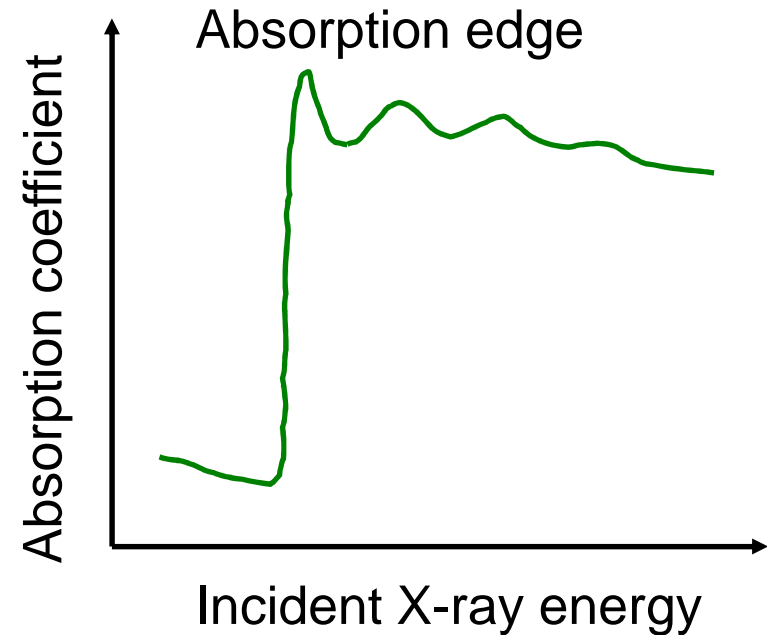
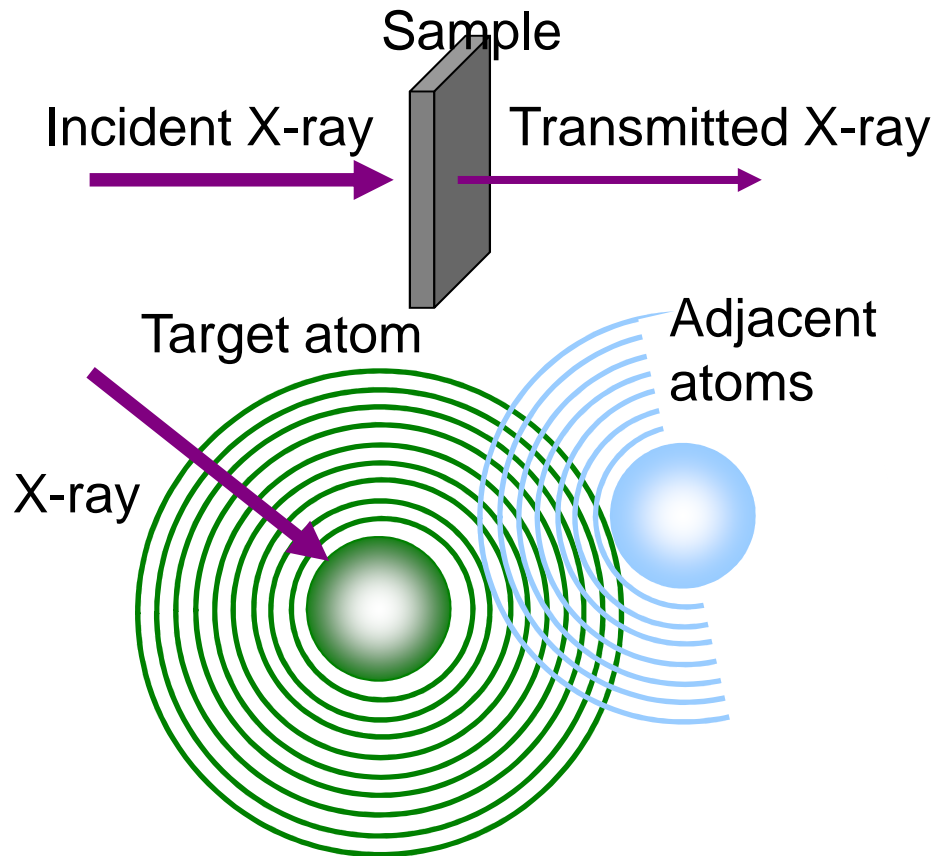


ZB-(Ga,Mn)As can be grown by selecting appropriate growth temperature

Highest Mn composition without segregation is about 10%.

A. Shen *et al.*, J. Cryst. Growth **175/176**, 1069 (1997).

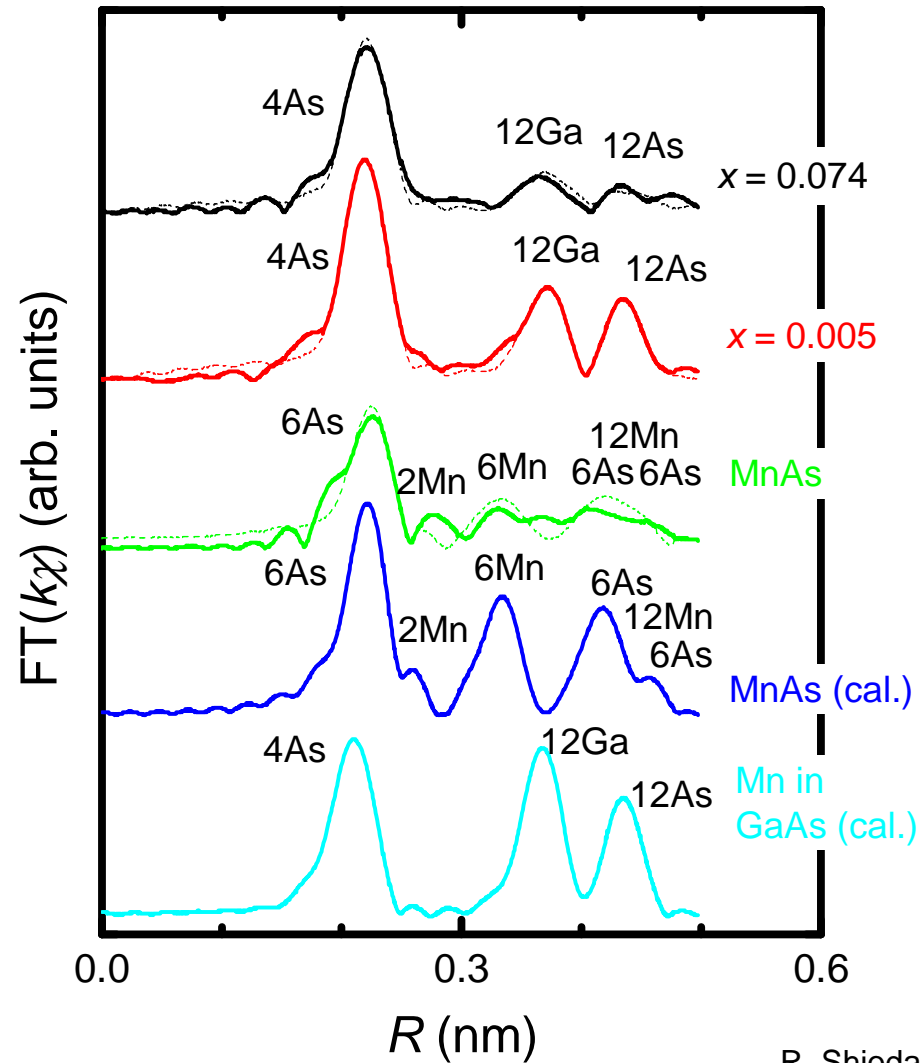
Extended X-ray-Absorption Fine Structure (EXAFS)



- X-ray is absorbed by target atom → creation of photoelectron
- Photoelectron is scattered by adjacent atoms
- Interference of photoelectron and reflected photoelectron
- Oscillating structure in absorption spectra includes the information of local structure around target atom

Local Structures - Extended X-ray-Absorption Fine Structure (EXAFS)

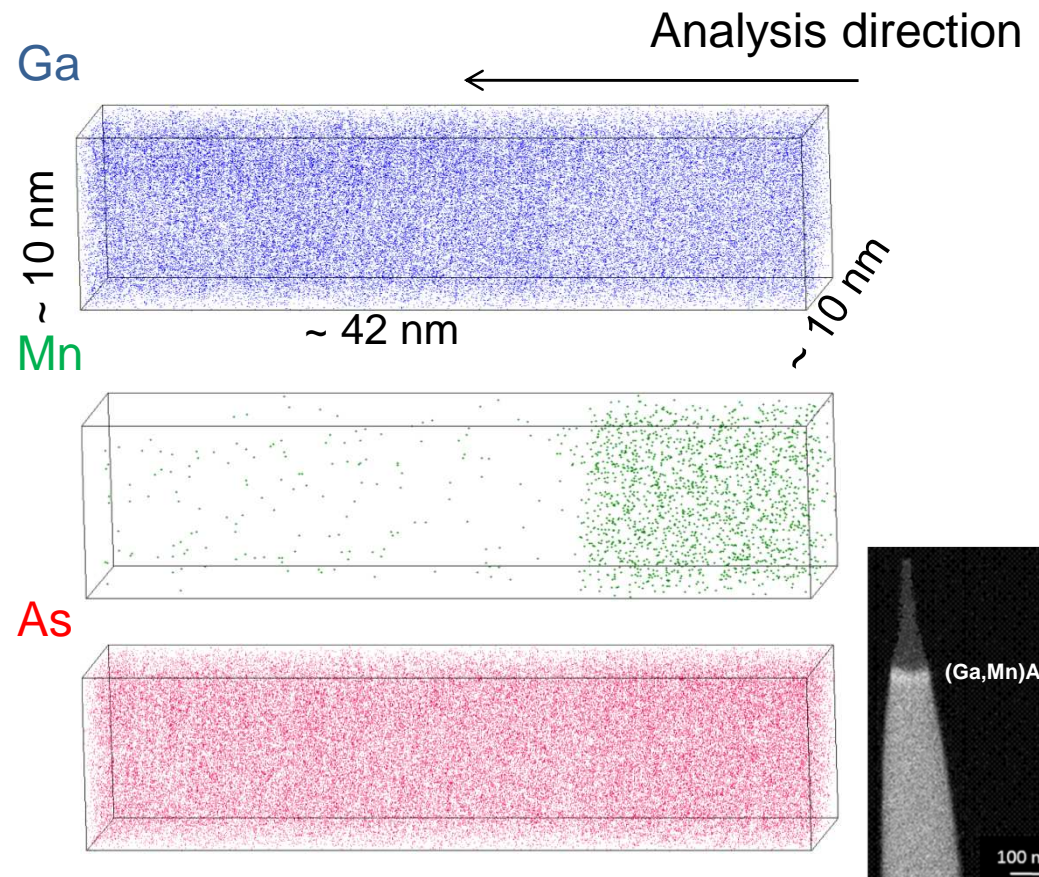
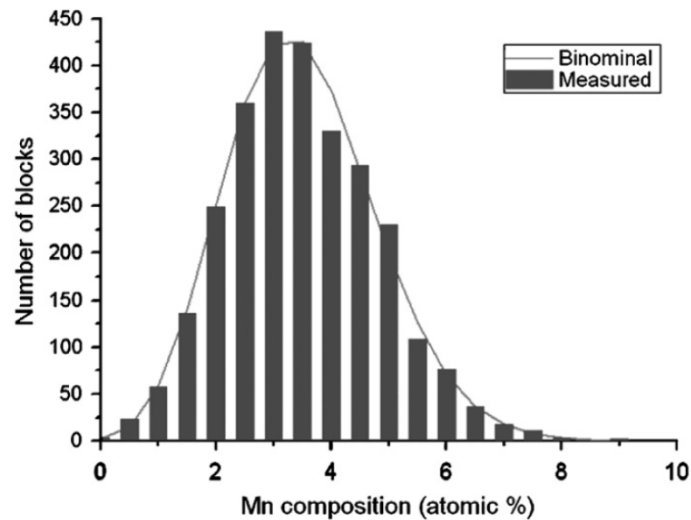
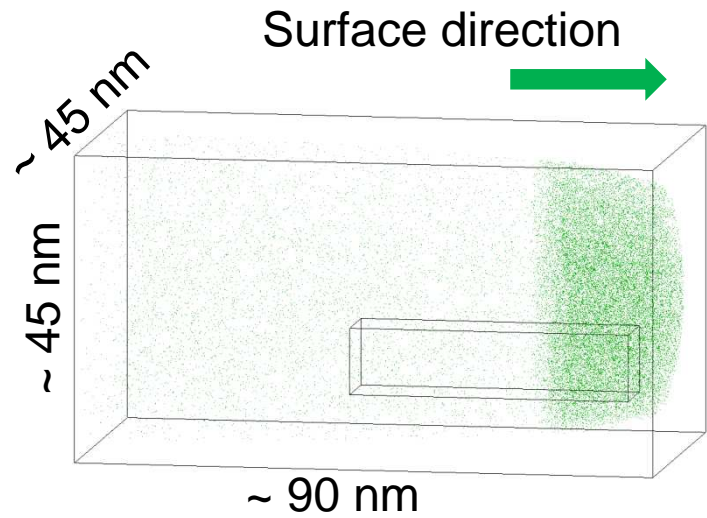
(Ga,Mn)As



R. Shioda *et al.*, Phys. Rev. B **58**, 1100 (1998).

Most of Mn substitute III-cation site ($Mn^{2+} \rightarrow$ acceptor)

Atom Probe Microscopy of (Ga,Mn)As

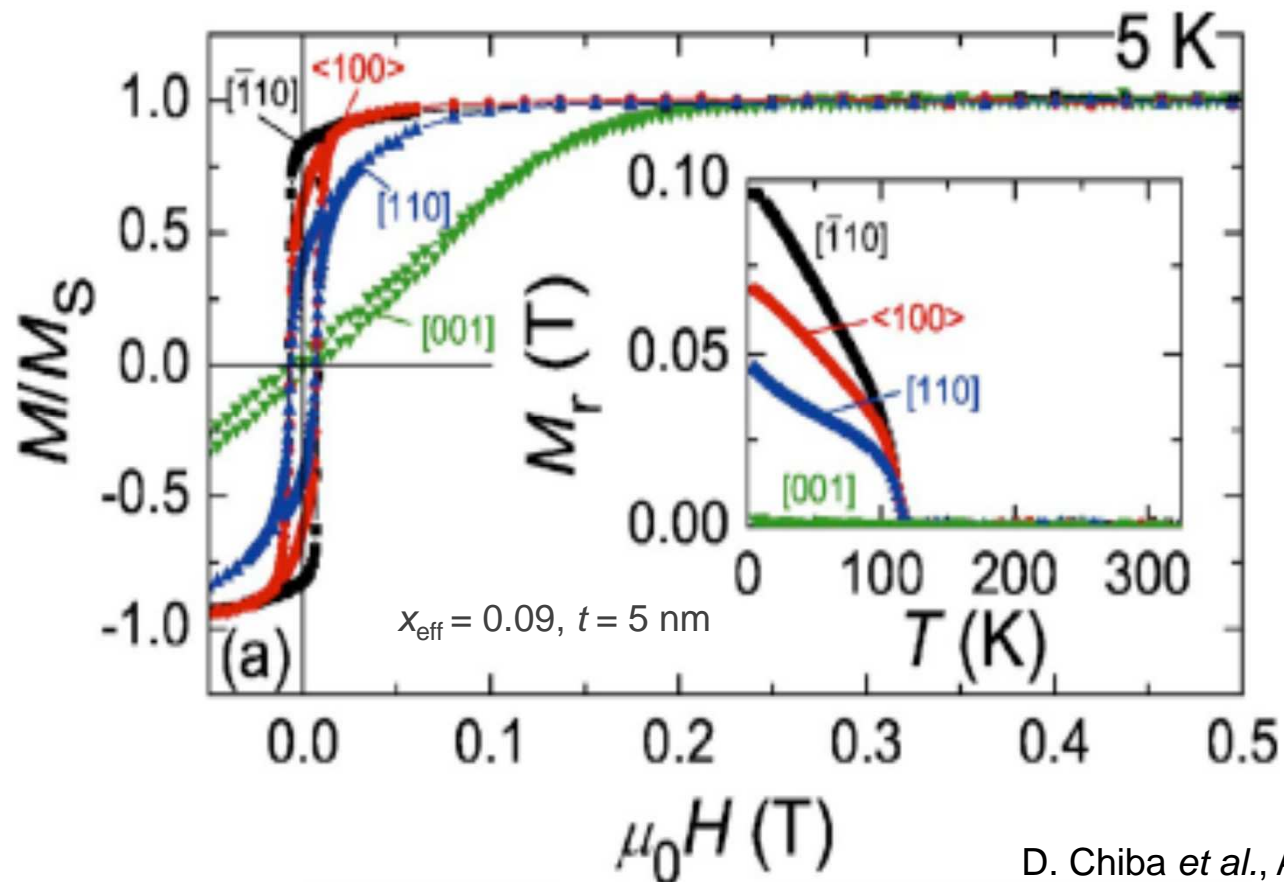


**Magnetism, transport,
and more materials science**

Magnetization of (Ga,Mn)As

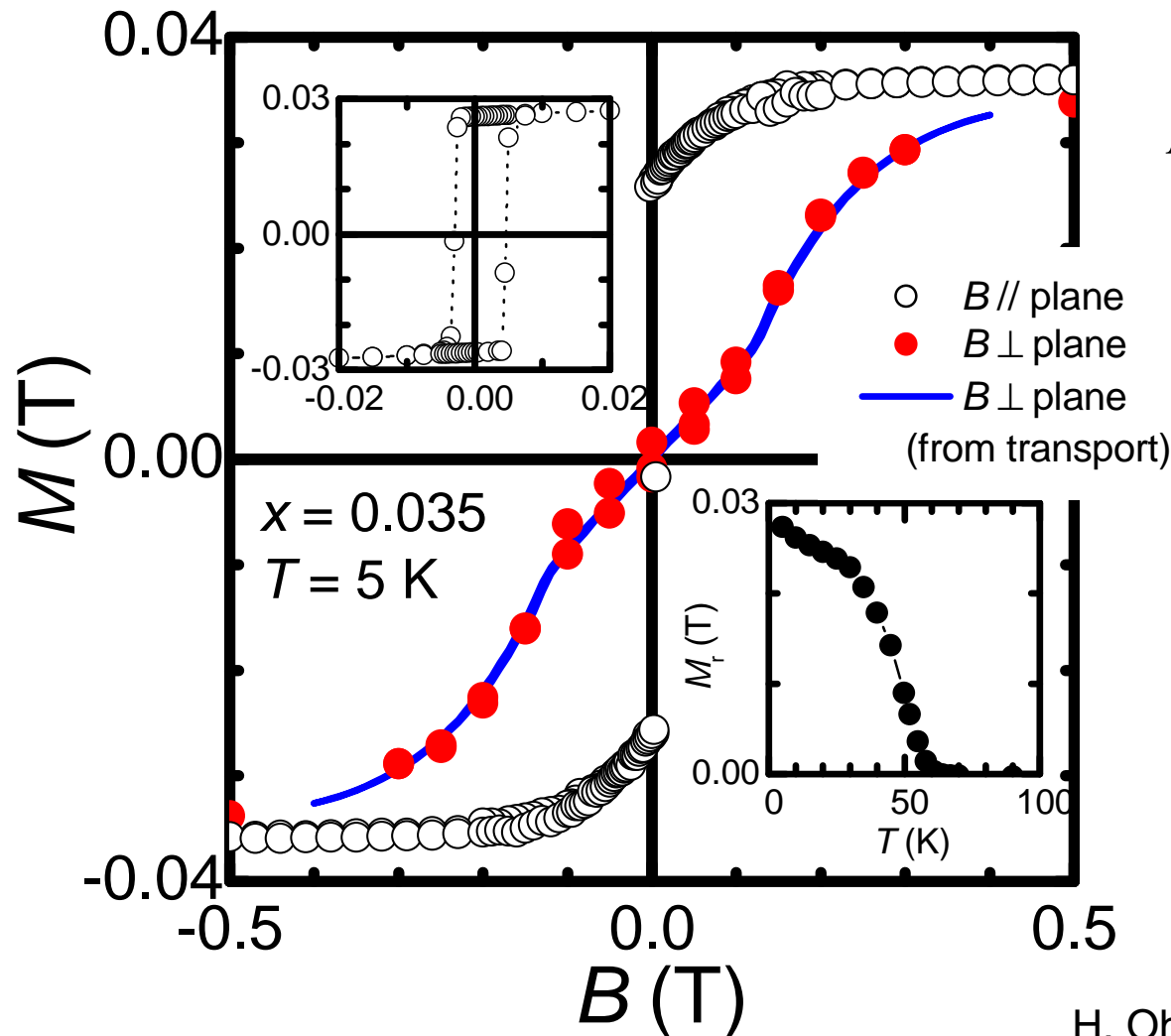
(Ga,Mn)As & (In,Mn)As: Mn acts as a source of spin and hole

Ferromagnetism in (In,Mn)As: H. Ohno *et al.*, *Phys Rev. Lett.* 1992
and in (Ga,Mn)As: H. Ohno *et al.*, *Appl. Phys. Lett.* 1996

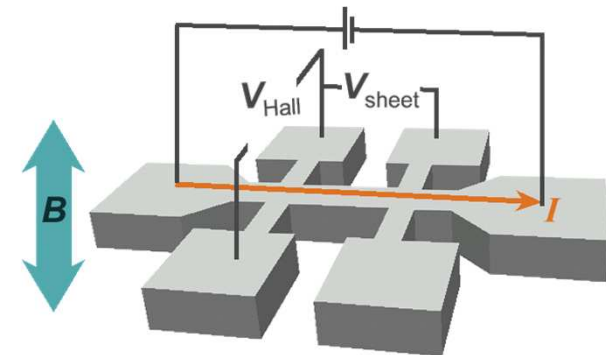


D. Chiba *et al.*, *APL* **90**, 122503 (2007)

Magnetization and transport of (Ga,Mn)As



$$R_{\text{Hall}} = (R_0/d)B + (R_s/d)M_{\perp}$$



$$R_{\text{Hall}} = V_{\text{Hall}}/I$$

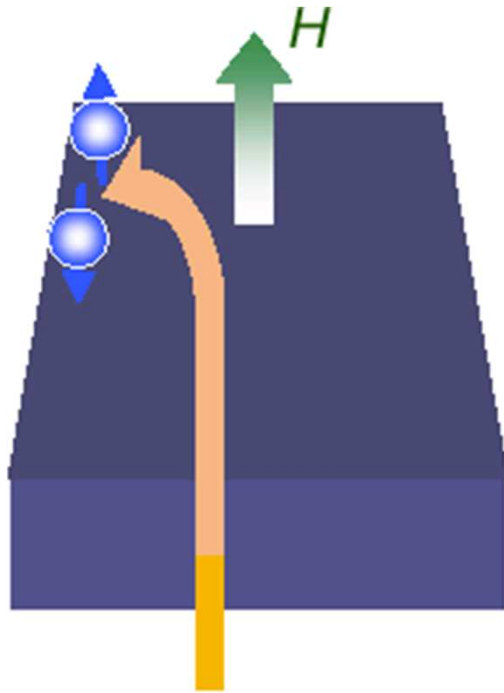
$$R_{\text{sheet}} \propto V_{\text{sheet}}/I$$

H. Ohno *et al.* *Appl. Phys. Lett.* 1996

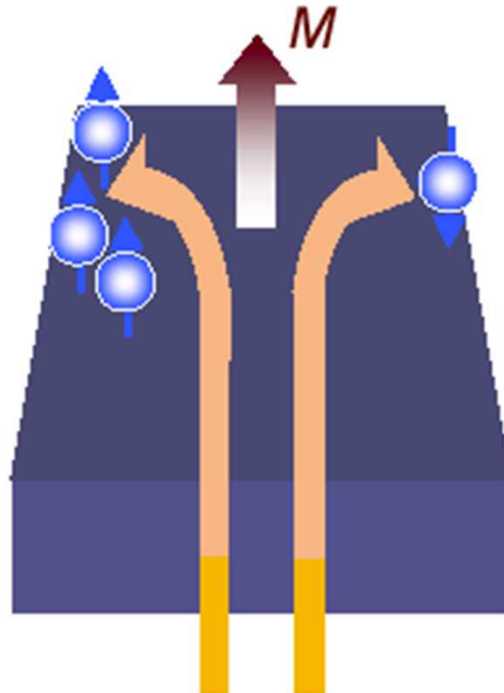
H. Ohno *Science* 1998

Hall Effects

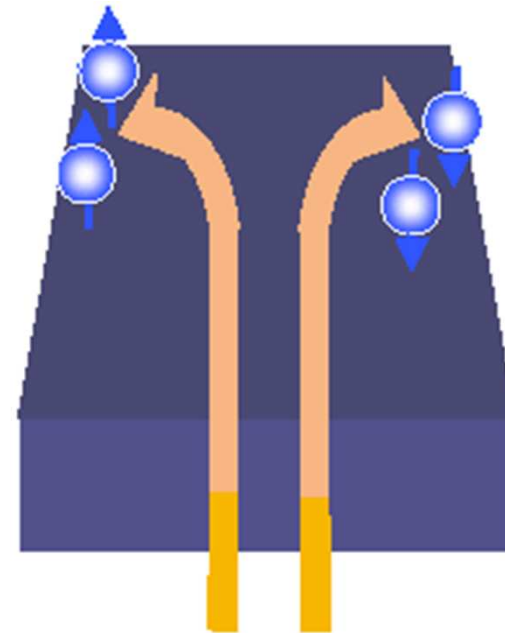
Ordinary Hall effect



Anomalous Hall effect



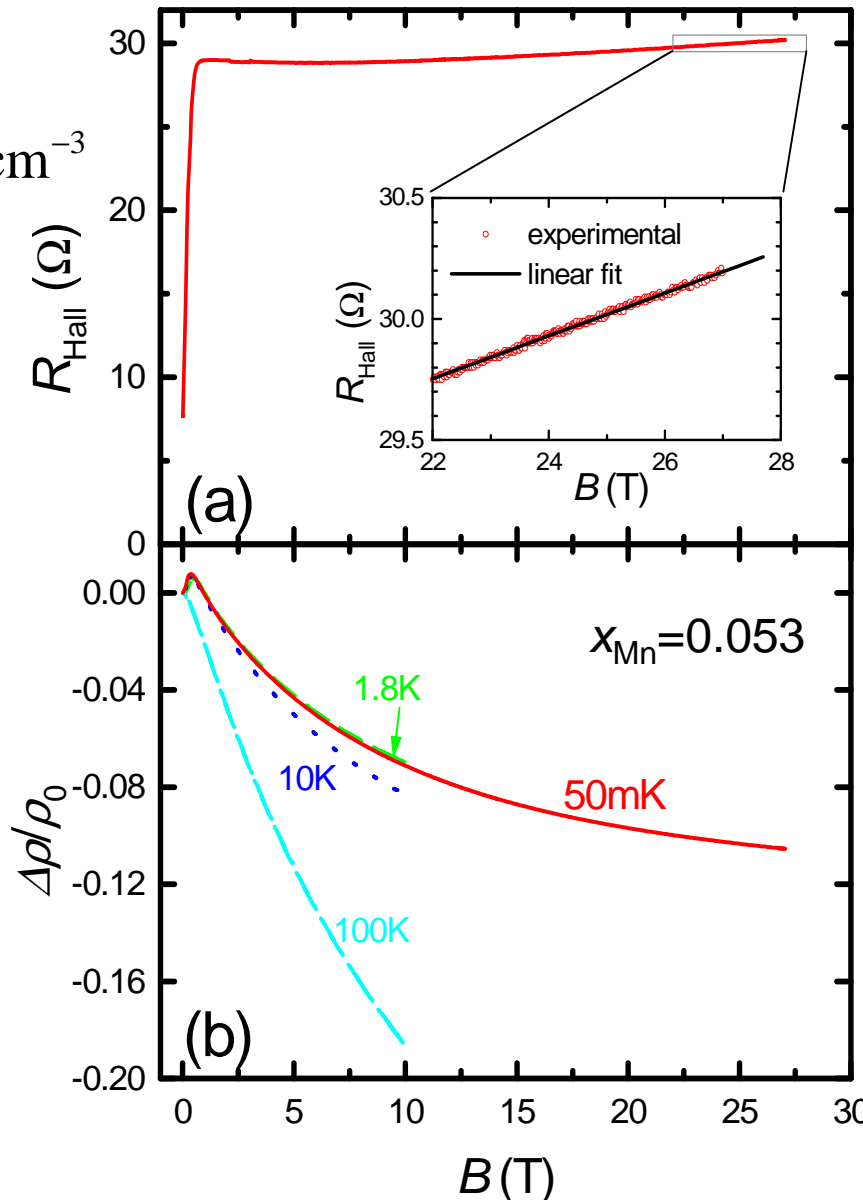
Spin Hall effect



Low-temperature & high-field measurements



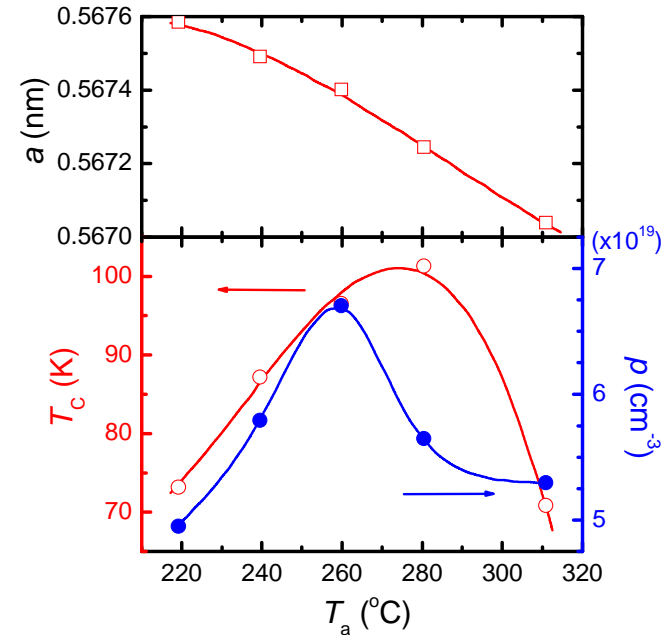
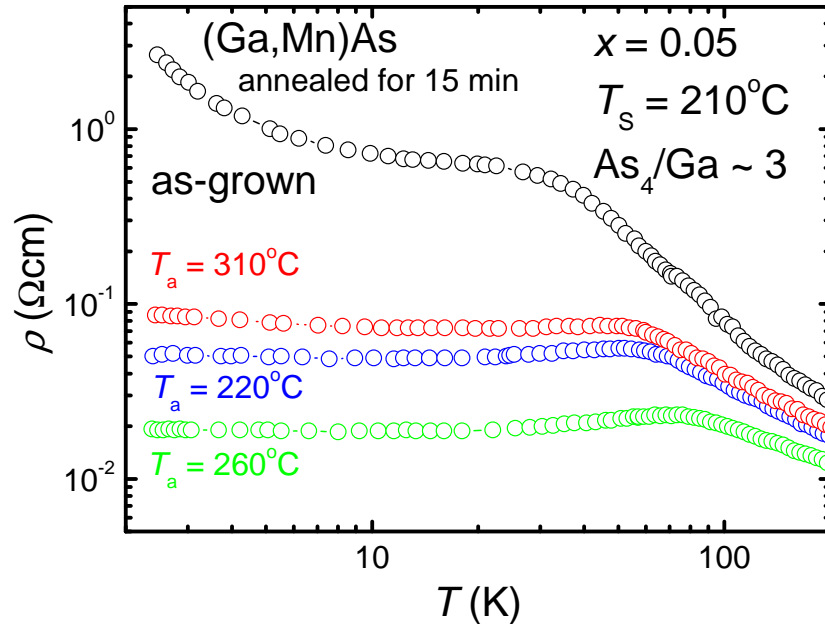
$[\text{Mn}] = 1.2 \times 10^{21} \text{ cm}^{-3}$



$\rho = 3.5 \times 10^{20} \text{ cm}^{-3}$
(30% of Mn)

$$\begin{aligned} \Delta\rho_{\text{Hall}} &= \Delta(R_0 B + R_S M_{\perp}) \\ &\approx R_0 \Delta B \\ &= \frac{1}{qpd} \Delta B \end{aligned}$$

Low-temperature annealing



T. Hayashi *et al.*, Appl. Phys. Lett. **78**, 1691 (2001).

Low-temperature annealing 220-250°C

- Decreases lattice constant
- Increases electrical conductivity
- Increases hole concentration
- Increases ferromagnetic transition temperature

Mn_i

Correlation between T_C and p

See also K. W. Edmonds *et al.*, Appl. Phys. Lett. **81**, 4991 (2002).

Ferromagnetism

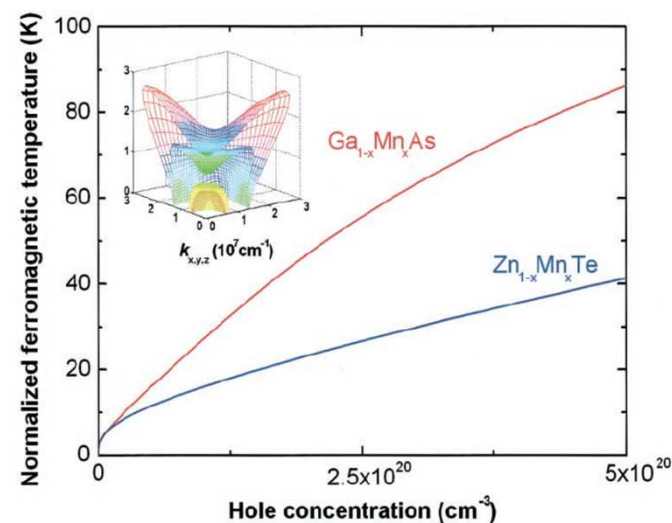
Zener Model Description of Ferromagnetism in Zinc-Blende Magnetic Semiconductors

T. Dietl,^{1,2*} H. Ohno,^{1*} F. Matsukura,¹ J. Cibert,³ D. Ferrand³

Ferromagnetism in manganese compound semiconductors not only opens prospects for tailoring magnetic and spin-related phenomena in semiconductors with a precision specific to III-V compounds but also addresses a question about the origin of the magnetic interactions that lead to a Curie temperature (T_C) as high as 110 K for a manganese concentration of just 5%. Zener's model of ferromagnetism, originally proposed for transition metals in 1950, can explain T_C of $\text{Ga}_{1-x}\text{Mn}_x\text{As}$ and that of its II-VI counterpart $\text{Zn}_{1-x}\text{Mn}_x\text{Te}$ and is used to predict materials with T_C exceeding room temperature, an important step toward semiconductor electronics that use both charge and spin.

SCIENCE VOL 287 11 FEBRUARY 2000

1019



Like other thermodynamic quantities, $F_c[M]$ is expected to be weakly perturbed by static disorder

We suggest that the holes in the extended or weakly localized states mediate the long-range interactions between the localized spins on both sides of the MIT in the III-V and II-VI magnetic semiconductors.

Visualizing Critical Correlations Near the Metal-Insulator Transition in $\text{Ga}_{1-x}\text{Mn}_x\text{As}$

Anthony Richardella,^{1,2*} Pedram Roushan,^{1*} Shawn Mack,³ Brian Zhou,¹ David A. Huse,¹ David D. Awschalom,³ Ali Yazdani^{1†}

www.sciencemag.org SCIENCE VOL 327 5 FEBRUARY 2010

665

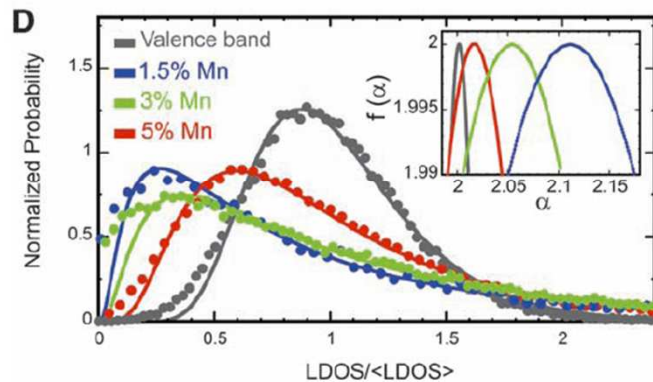
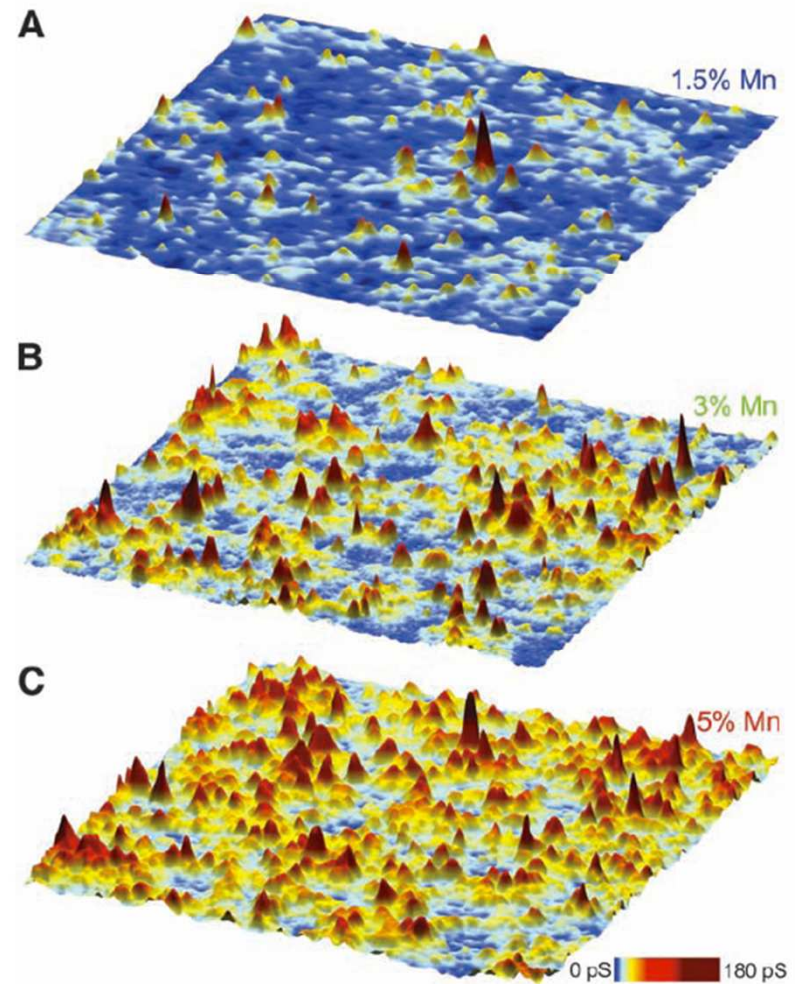


Fig. 5. The spatial variations of the LDOS at the Fermi level, with their histogram and multifractal spectrum. The LDOS mapping of a 700 Å by 700 Å area of (A) $\text{Ga}_{0.985}\text{Mn}_{0.015}\text{As}$, (B) $\text{Ga}_{0.97}\text{Mn}_{0.03}\text{As}$, and (C) $\text{Ga}_{0.95}\text{Mn}_{0.05}\text{As}$. (D) The normalized histogram of the maps presented in (A) to (C). The local values of the dI/dV are normalized by the average value of each map. The inset shows the multifractal spectrum, $f(\alpha)$, near the value α_0 where the maximum value occurs. For comparison, the results of a similar analysis over a LDOS map at -100 mV (valence band states) for the 1.5% doped sample are also shown.



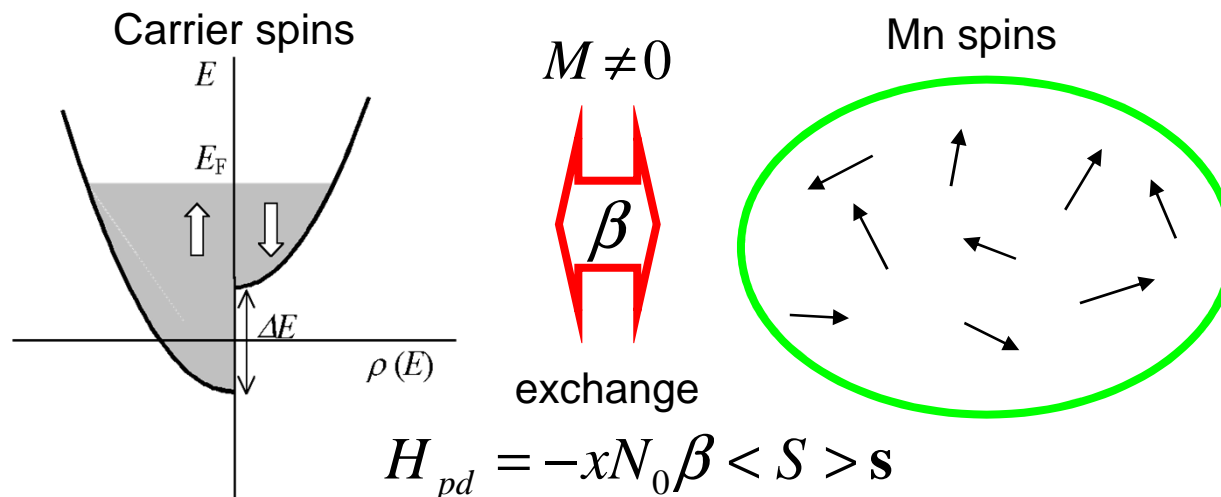
p-d Zener model of ferromagnetism

Ferromagnetic (Ga,Mn)As

Mn acts as a source of spin and hole

H. Ohno *et al. Appl. Phys. Lett.* 1996

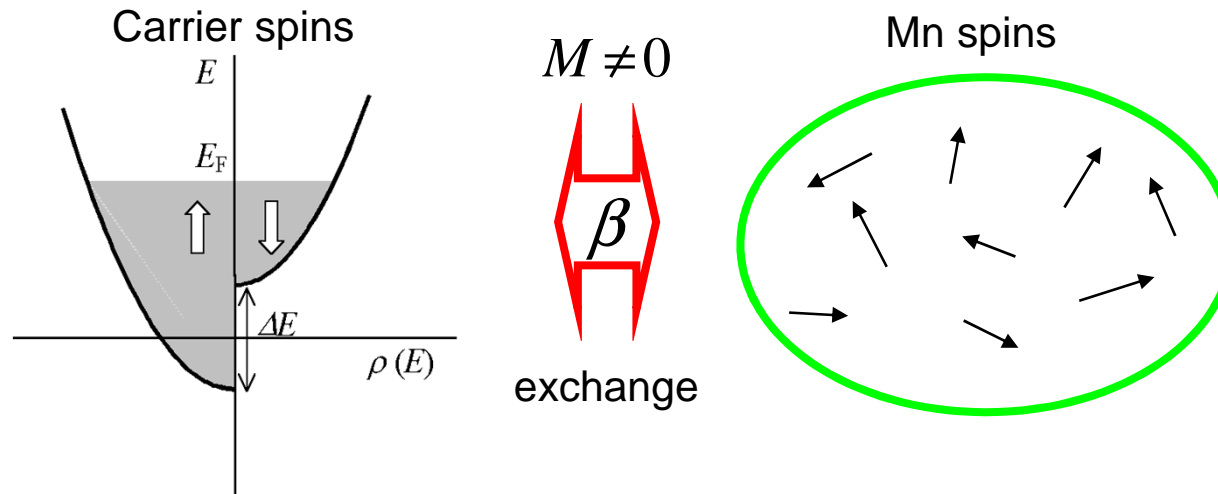
H. Ohno *Science* 1998



$$T_c = \frac{xN_0 S(S+1)A_F \rho(E_F) \beta^2}{12k_B}$$

T. Dietl, *et al. Science* **287**, 1019 (2000) and *PRB* **63**, 195205 (2001)
also Koenig *et al. Phys. Rev. Lett.* 2000

T_C by the p - d Zener model

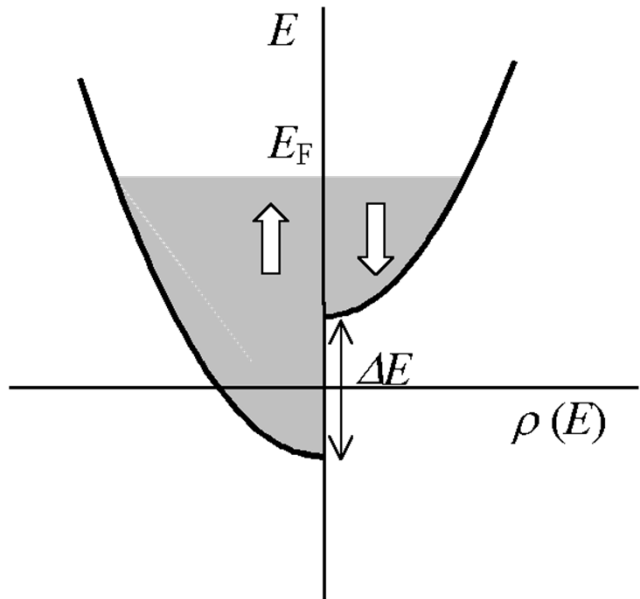


$$\begin{aligned}\Delta F_{total} &= \Delta F_{Mn} + \Delta F_c \\ &= \frac{M^2}{2\chi_{Mn}} - \frac{\chi_c}{2} H^2\end{aligned}$$

$$\chi_{Mn} = \frac{g^2 \mu_B^2 x N_0 S(S+1)}{3k_B T}$$

$$\chi_c = \mu_B^2 \rho(E_F)$$

T_c by the p - d Zener model



$$\Delta E = 2\mu_B H$$

$$\Delta E = xN_0 |\beta \langle S \rangle|$$

$$M = xN_0 g \mu_B |\langle S \rangle|$$

$$\Delta E = \frac{|\beta| M}{g \mu_B}$$

$$\left. \begin{aligned} \Delta E &= 2\mu_B H \\ \Delta E &= xN_0 |\beta \langle S \rangle| \\ M &= xN_0 g \mu_B |\langle S \rangle| \end{aligned} \right\} \begin{aligned} H &= \frac{\Delta E}{2\mu_B} \\ &= \frac{|\beta| M}{2g\mu_B^2} \end{aligned}$$

$$\Delta F_{total} = \frac{M^2}{2\chi_{Mn}} - \frac{\chi_c}{2} H^2$$

$$= \left(\frac{1}{2 \left(\frac{g^2 \mu_B^2 x N_0 S(S+1)}{3k_B T} \right)} - \frac{\rho(E_F) \beta^2}{8g^2 \mu_B^2} \right) M^2$$

$$T_c = \frac{xN_0 S(S+1) \rho(E_F) \beta^2}{12k_B}$$

$$\Delta F_c(M) \approx -\frac{A_F \rho(E_F) \beta^2}{8g^2 \mu_B^2} M^2$$

Valence band structure (Γ_7, Γ_8)

$$H_{kp} \Psi = E \Psi$$

Basis functions

$$u_1 = \frac{1}{\sqrt{2}}(X + iY) \uparrow, \quad u_2 = i \frac{1}{\sqrt{6}}[(X + iY) \downarrow - 2Z \uparrow], \quad u_3 = \frac{1}{\sqrt{6}}[(X - iY) \uparrow + 2Z \downarrow],$$

$$u_4 = i \frac{1}{\sqrt{2}}(X - iY) \downarrow, \quad u_5 = \frac{1}{\sqrt{3}}[(X + iY) \downarrow + Z \uparrow], \quad u_6 = i \frac{1}{\sqrt{3}}[-(X - iY) \uparrow + Z \downarrow]$$

$k \cdot p$ matrix

$$H_{kp} = -\frac{\hbar^2}{2m_0} \begin{pmatrix} P+Q & L & M & 0 & iL/\sqrt{2} & -i\sqrt{2}M \\ L^\dagger & P-Q & 0 & M & -i\sqrt{2}Q & i\sqrt{3/2}L \\ M^\dagger & 0 & P-Q & -L & -i\sqrt{3/2}L^\dagger & -i\sqrt{2}Q \\ 0 & M^\dagger & -L^\dagger & P+Q & -i\sqrt{2}M^\dagger & -iL^\dagger/\sqrt{2} \\ -iL^\dagger/\sqrt{2} & i\sqrt{2}Q & i\sqrt{3/2}L & i\sqrt{2}M & P+\Delta & 0 \\ i\sqrt{2}M^\dagger & -i\sqrt{3/2}L^\dagger & i\sqrt{2}Q & iL/\sqrt{2} & 0 & P+\Delta \end{pmatrix}$$

$$P = \gamma_1 k^2, \quad Q = \gamma_2 (k_x^2 + k_y^2 - 2k_z^2), \quad L = -2\sqrt{3}\gamma_3 (k_x - ik_y)k_z, \quad M = -\sqrt{3}[\gamma_2 (k_x^2 - k_y^2) - 2i\gamma_3 k_x k_y]$$

$$\gamma_1 = 6.85, \quad \gamma_2 = 2.1, \quad \gamma_3 = 2.58, \quad \Delta = 0.34 \text{ eV for GaAs}$$

Valence band structure with p - d exchange (Γ_7, Γ_8)

$$(H_{kp} + H_{pd})\Psi = E\Psi$$

p - d exchange interaction matrix

$$H_{pd} = B \cdot \begin{pmatrix} 3b_x w_z & i\sqrt{3}b_x w_- & 0 & 0 & \sqrt{6}b_x w_- & 0 \\ -i\sqrt{3}b_x w_+ & (2b_z - b_x)w_z & 2ib_z w_- & 0 & i\sqrt{2}(b_x + b_z)w_z & \sqrt{2}b_z w_- \\ 0 & -2ib_z w_+ & -(2b_z - b_x)w_z & i\sqrt{3}b_x w_- & \sqrt{2}b_z w_+ & -i\sqrt{2}(b_x + b_z)w_z \\ 0 & 0 & -i\sqrt{3}b_x w_+ & -3b_x w_z & 0 & -\sqrt{6}b_x w_+ \\ \sqrt{6}b_x w_+ & -i\sqrt{2}(b_x + b_z)w_z & \sqrt{2}b_z w_- & 0 & -(2b_x - b_z)w_z & ib_z w_- \\ 0 & 0 & i\sqrt{2}(b_x + b_z)w_z & -\sqrt{6}b_x w_- & -ib_z w_+ & (2b_x - b_z)w_z \end{pmatrix}$$

$$B = -\frac{1}{6} x N_0 \beta \langle S_z \rangle, \quad \beta_x = b_x \beta, \quad \beta_z = b_z \beta$$

$$w_z = \langle S_z \rangle / \langle S \rangle, \quad w_{\pm} = (\langle S_x \rangle \pm i \langle S_y \rangle) / \langle S \rangle$$

$$\langle S \rangle = \left| \langle S_x \rangle^2 + \langle S_y \rangle^2 + \langle S_z \rangle^2 \right|^{1/2}$$

Exchange energy: $N_0\beta$

Core level photoemission and modeling:

$$N_0\beta = -1.2 \pm 0.2 \text{ eV}$$

Okabayashi et al., Phys. Rev. B58, 1998.

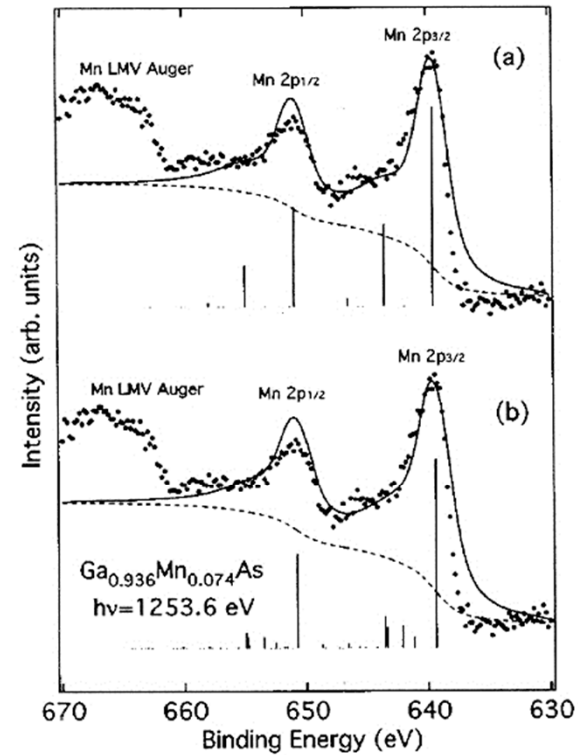
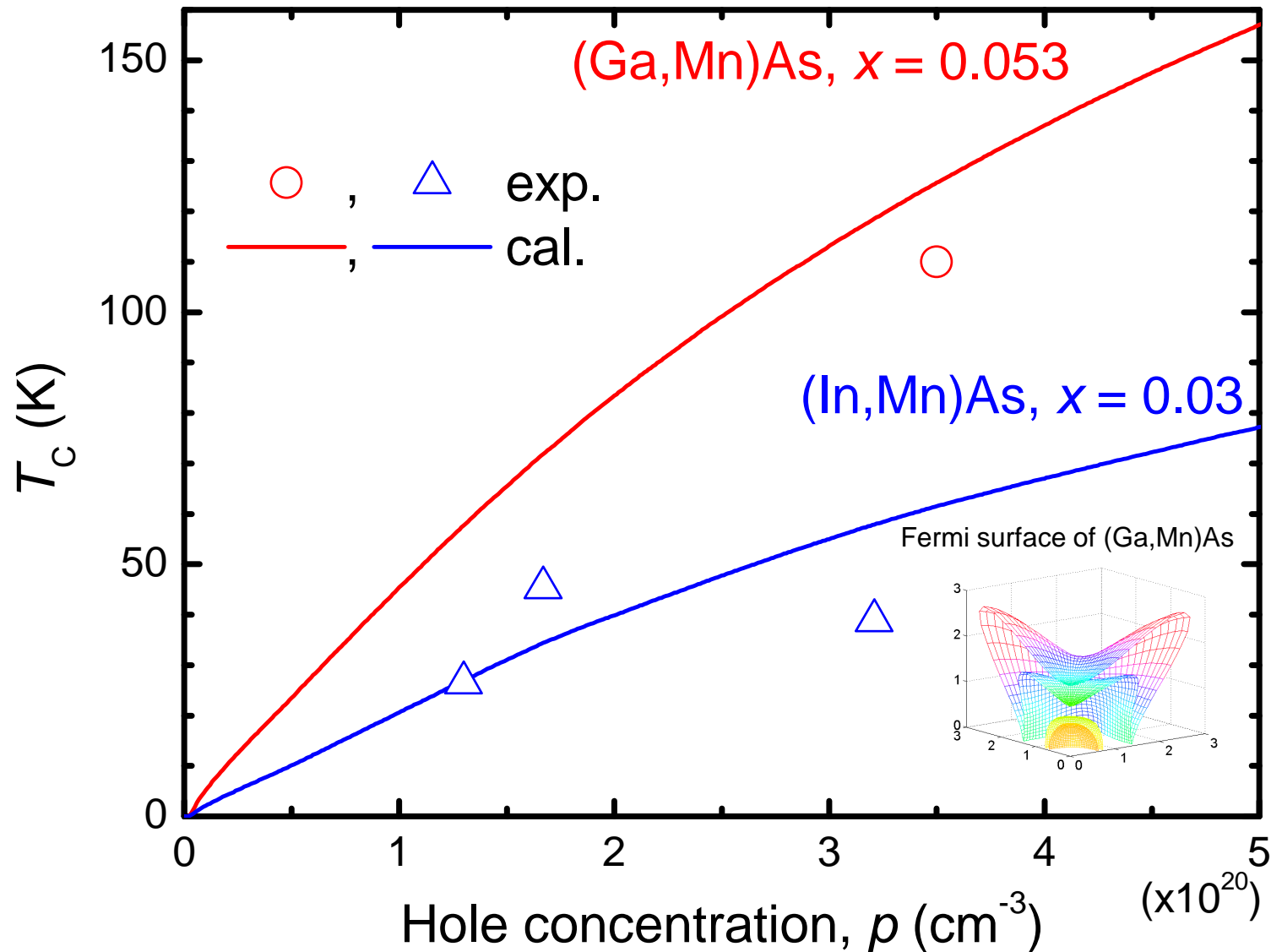
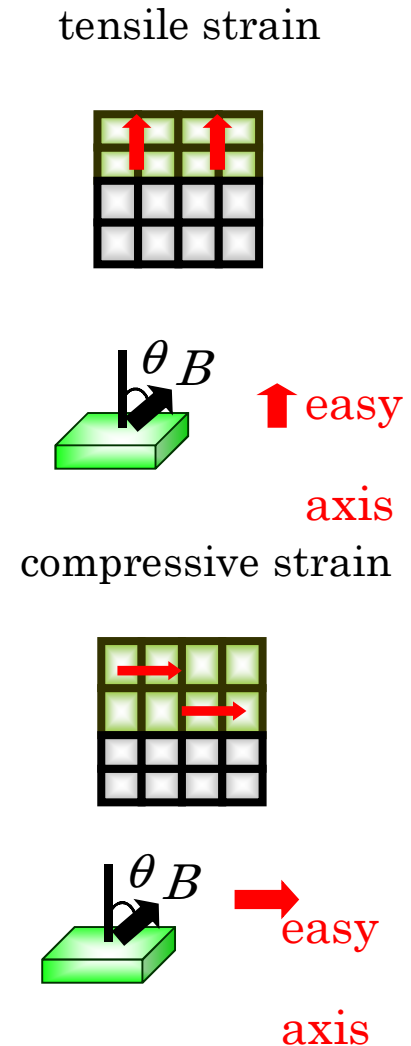
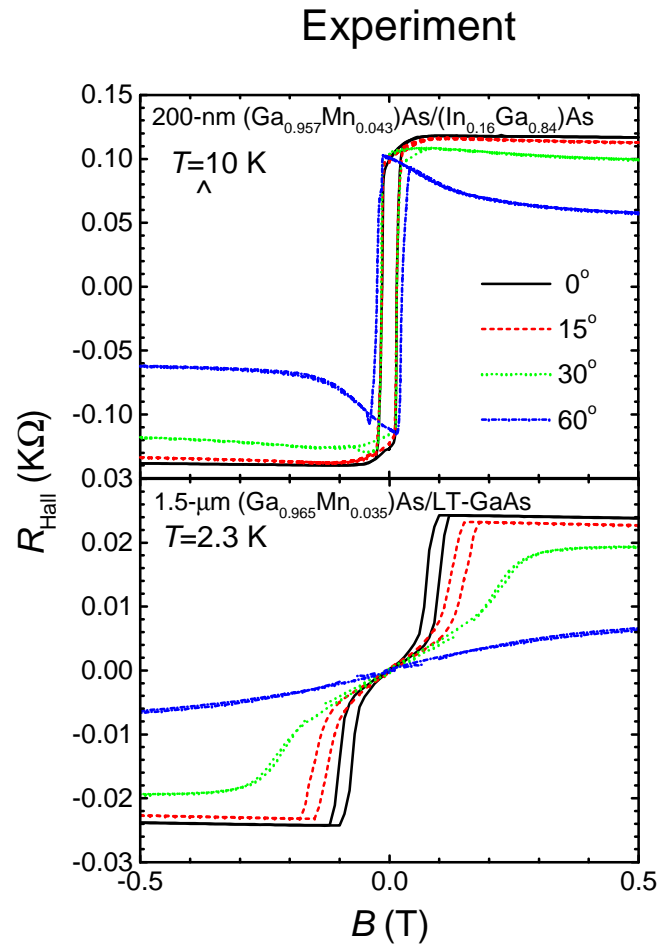
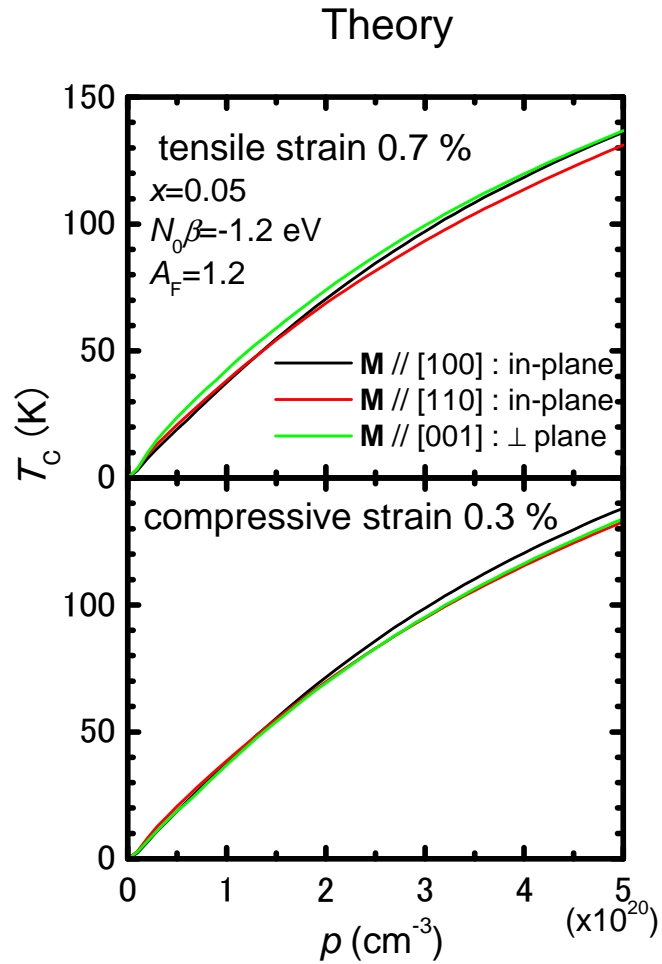


FIG. 1. Photoemission spectrum of the Mn 2p core level (dots) and its cluster-model analysis (solid curves) assuming the negatively ionized Mn²⁺ (a) and neutral Mn³⁺ (b) ground states. The vertical bars are unbroadened spectra. The calculated background is shown by dashed curves.

Comparison of exp. and calculated T_C

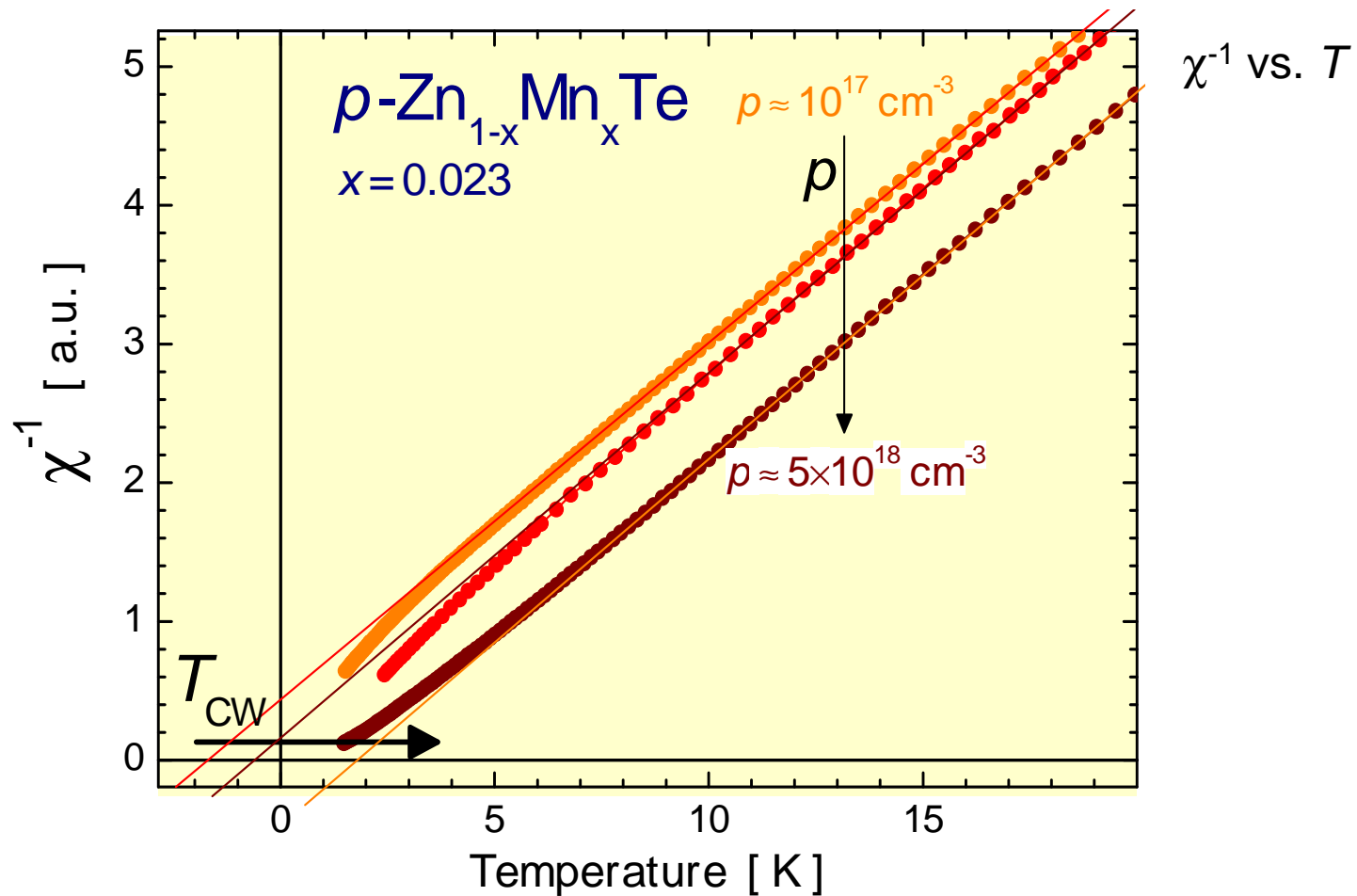


Strain induced-anisotropy: Theory vs. Experiment



Hole bands are responsible for the anisotropy

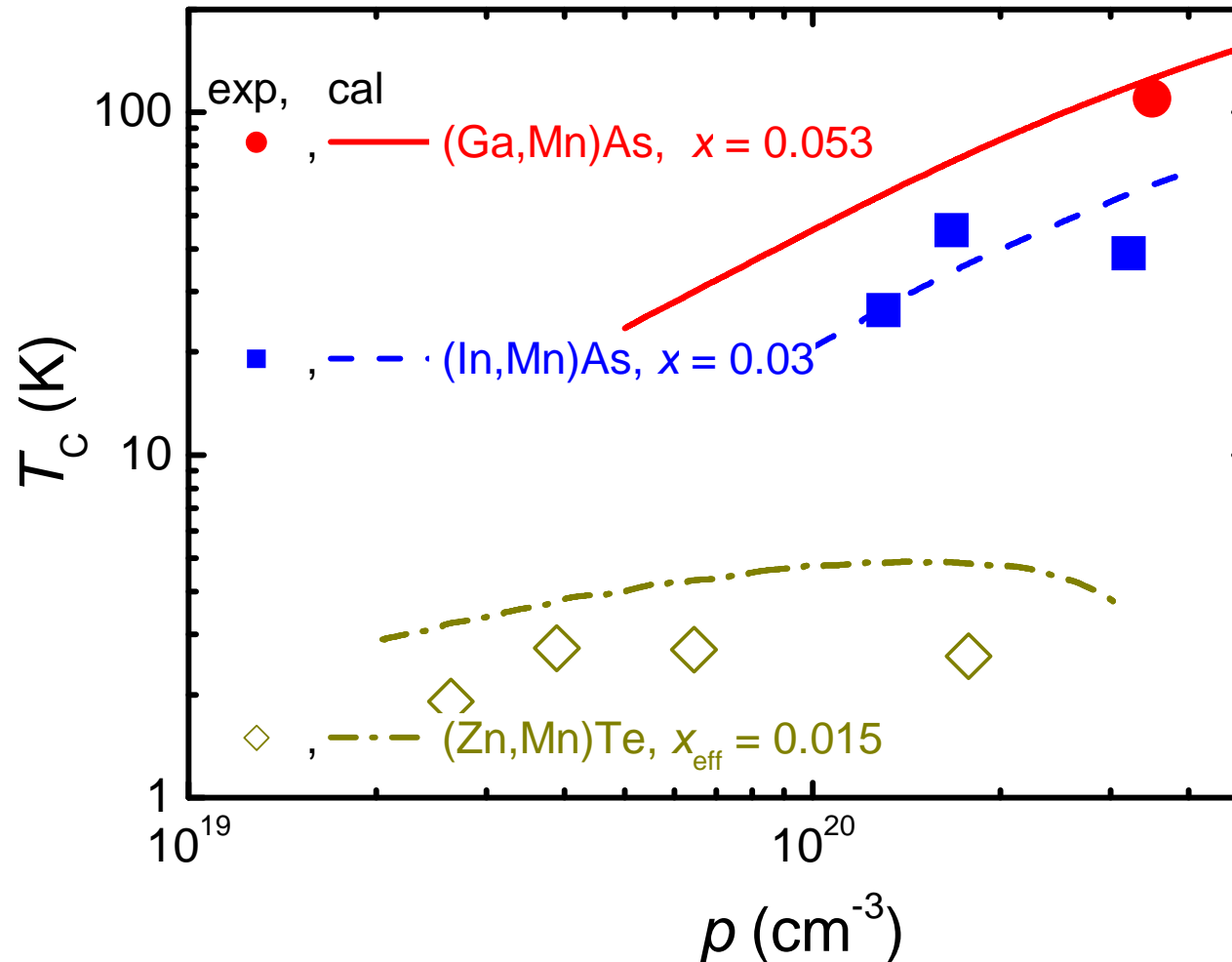
Acceptor doping and susceptibility of $\text{Zn}_{1-x}\text{Mn}_x\text{Te:P}$



Sawicki et al. (Warsaw) pss'02

Kępa et al. (Warsaw, Oregon) PRL'03

Comparison of Experimental and Calculated T_C

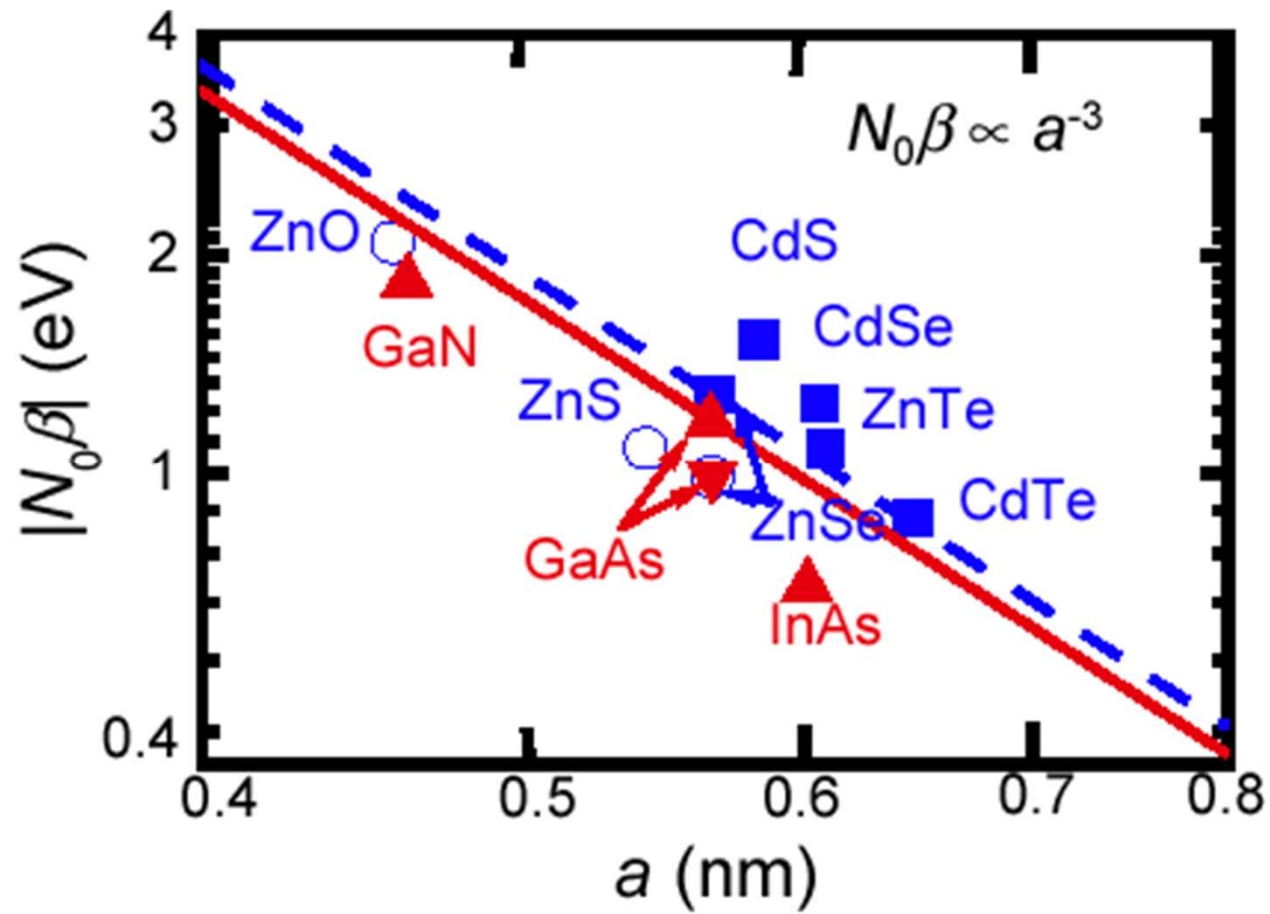


exp.: (Ga,Mn)As: T. Omiya *et al.*, Physica E **7**, 976 (2000).

(In,Mn)As: D. Chiba *et al.*, J. Supercond. and Novel Mag. **16**, 179 (2003).

(Zn,Mn)Te: D. Ferrand *et al.*, Phys. Rev. B **63**, 085201 (2001).

p-d exchange energy



4. Making “use” of ferromagnetism in semiconductors

- **Electrical control of ferromagnetism**
- **Current induced domain wall motion**
- **Tunneling with magnetism**

commentary

A window on the future
of spintronics

Hideo Ohno

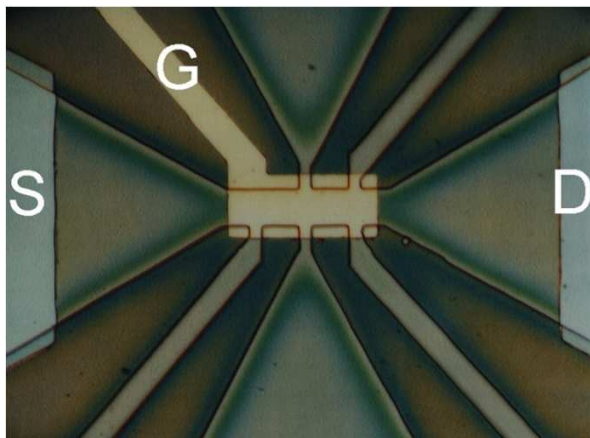
4. Making “use” of ferromagnetism in semiconductors

- **Electrical control of ferromagnetism**
- Current induced domain wall motion
- Tunneling with magnetism

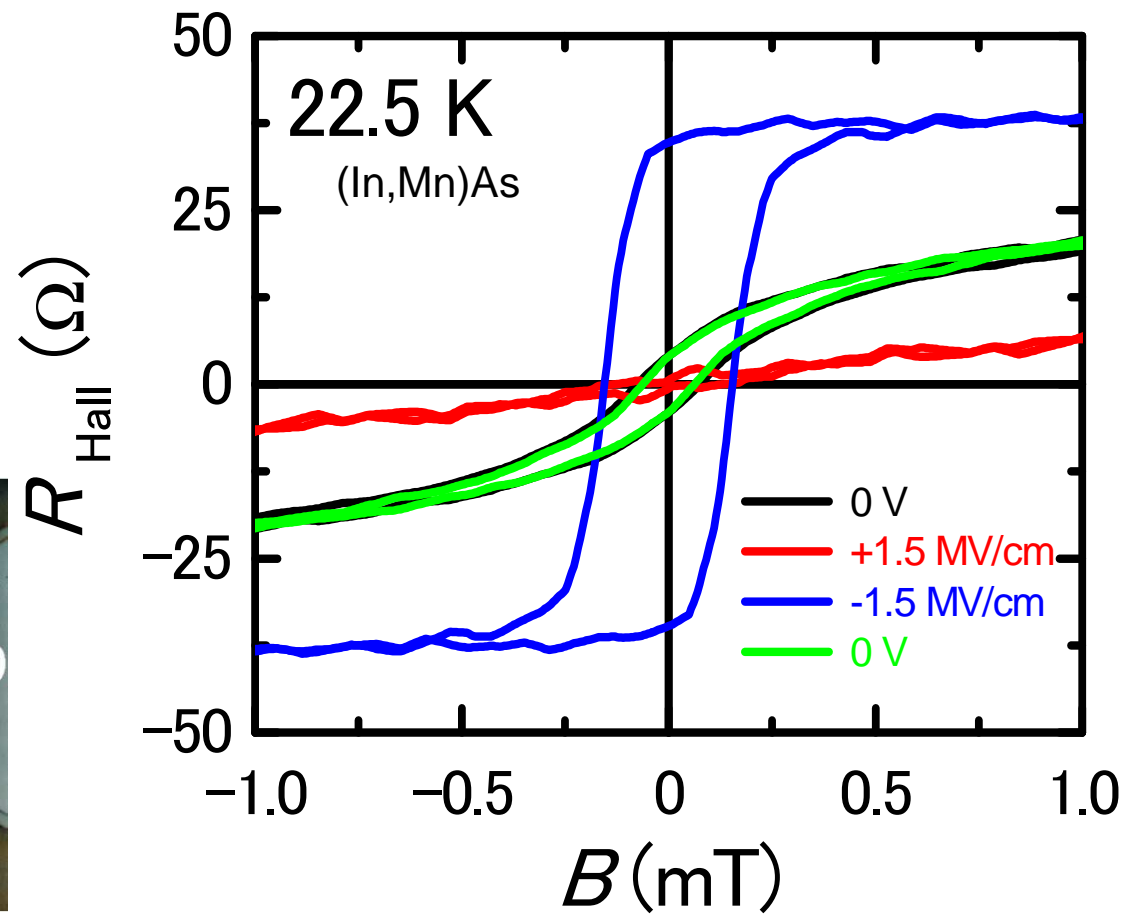
Electric-field control of ferromagnetism

(In,Mn)As

95/5 nm	Au/Cr
800 nm	polyimide
5 nm	(In _{0.97} Mn _{0.03})As
10 nm	InAs
400 nm	(Al _{0.6} Ga _{0.4})Sb
100 nm	AlSb
	GaAs sub.

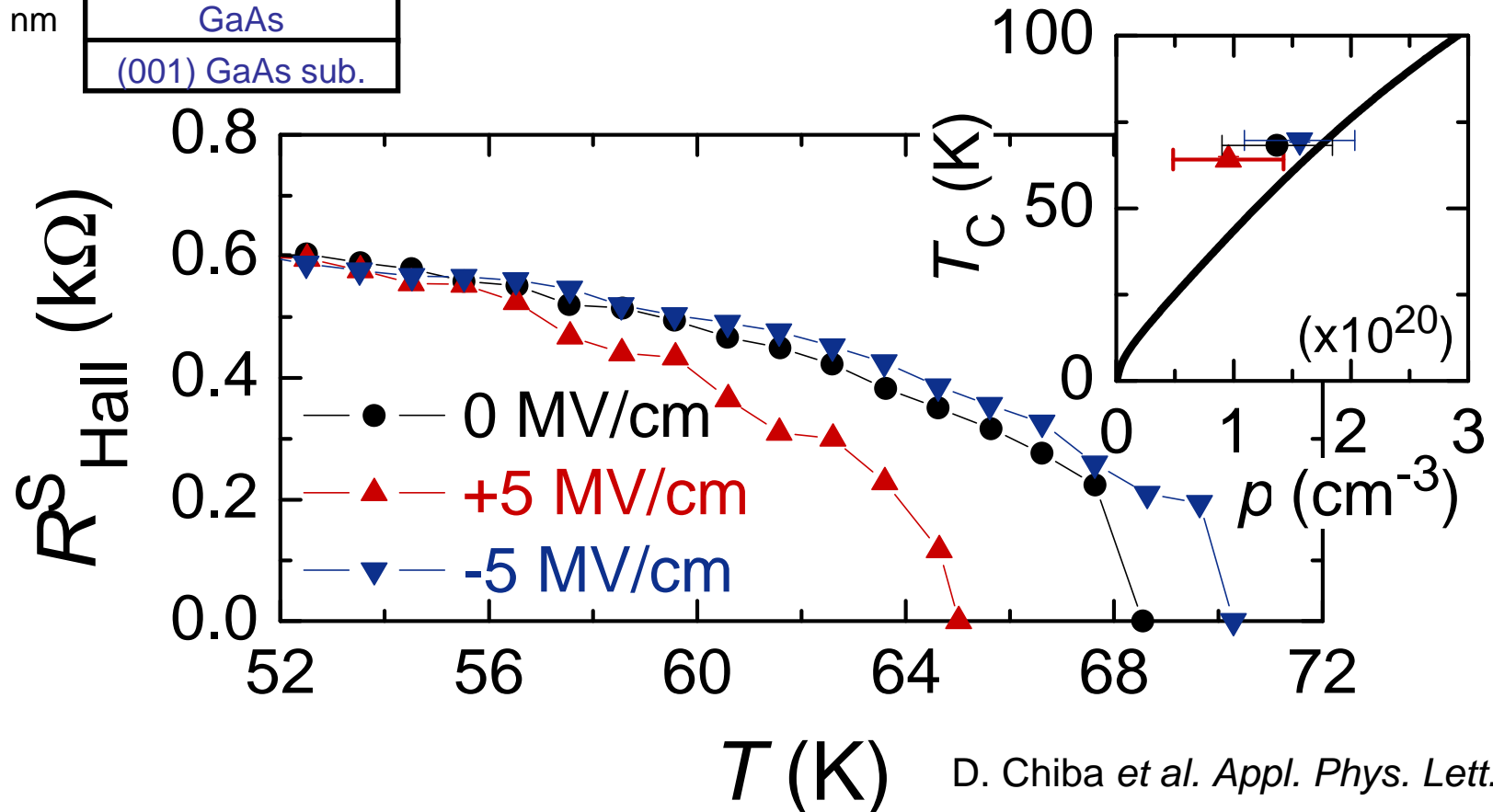


$$R_{\text{Hall}} = (R_0/d)B + (R_S/d)M_{\perp}$$



Electric-field control: the case of (Ga,Mn)As

100/5 nm	Au/Cr
50 nm	Al ₂ O ₃
7 nm	(Ga _{0.953} Mn _{0.047})A
30 nm	(Al _{0.80} Ga _{0.20})As
500 nm	(In _{0.13} Ga _{0.87})As
100 nm	GaAs
	(001) GaAs sub.

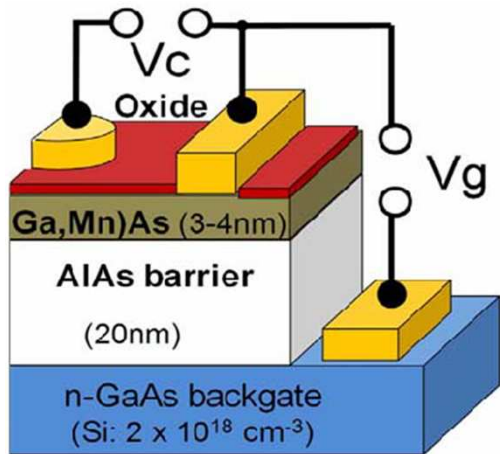


D. Chiba *et al.* *Appl. Phys. Lett.* 2006

See also Y. Nishitani *et al.*, *Phys. Rev. B* **81**, 045208 (2010) and M. Sawicki, *et al.*, *Nature Physics*, **6**, 22 (2010)

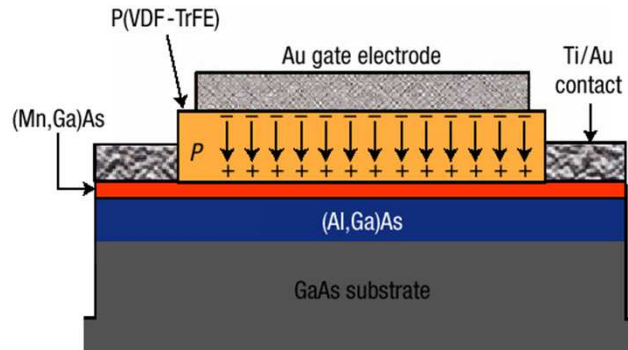
Field-effect structures of (Ga,Mn)As

backgate structure



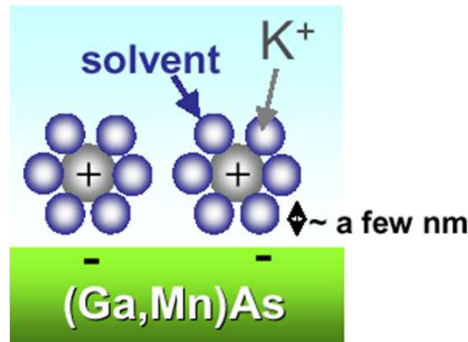
K. Olejník *et al.*,
 Phys. Rev. B **78**, 054403 (2008);
 M. S. H. Owen *et al.*, New J. Phys. **11**, 023008 (2009).

ferroelectric-gate structure



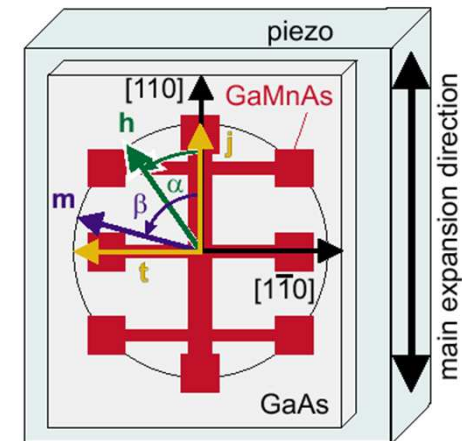
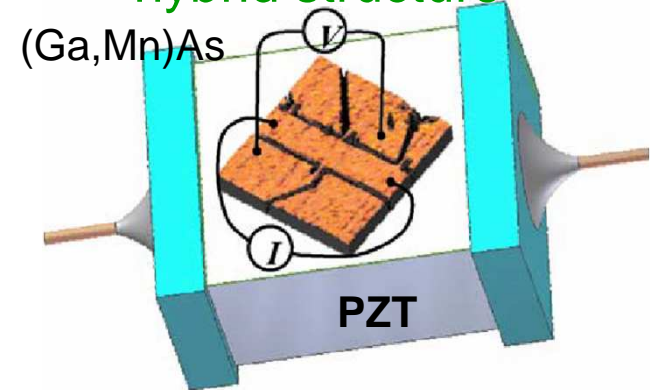
I. Stokichnov *et al.*, Nature Mater. **7**, 464 (2008).

electric double layer



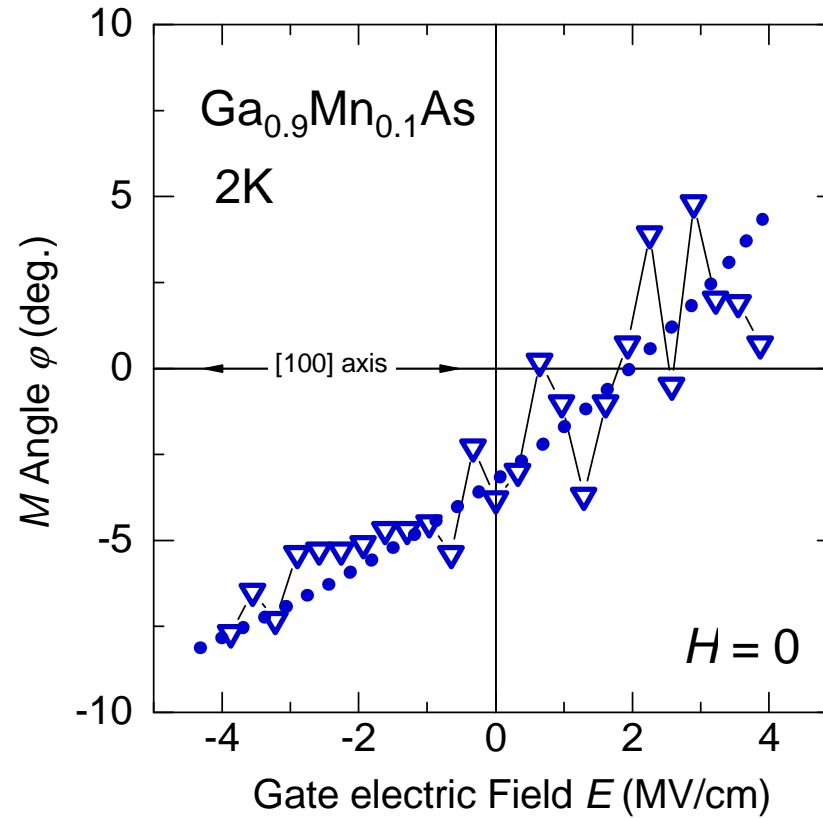
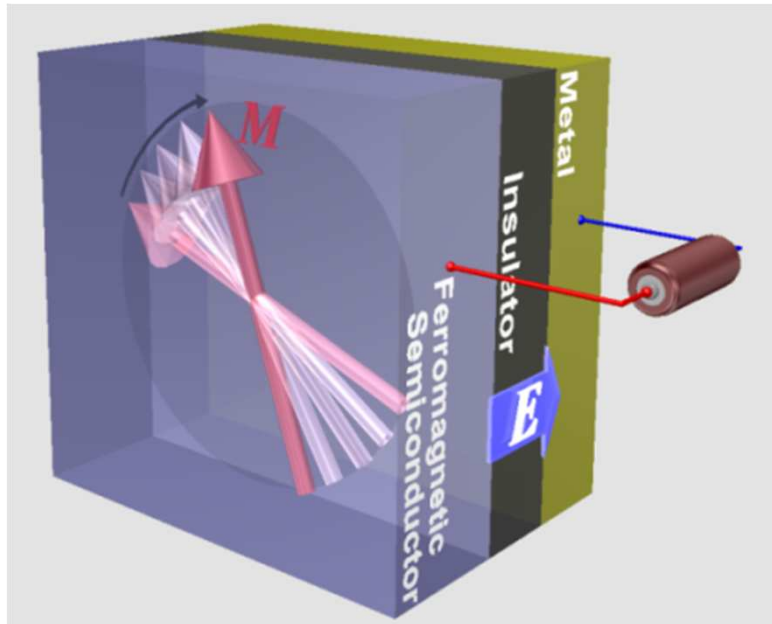
M. Endo *et al.*, Appl. Phys. Lett. **96**, 022515 (2010).

piezoelectric hybrid structure

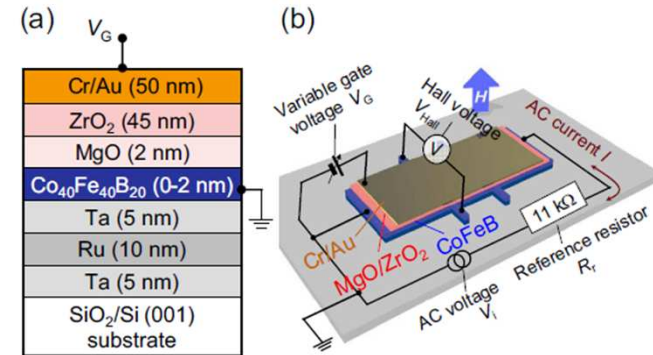
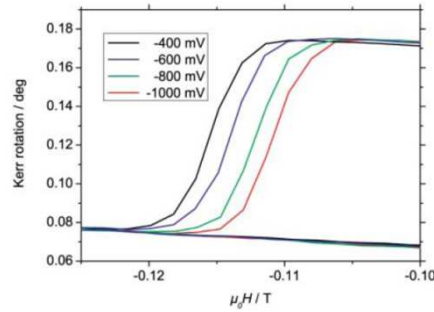
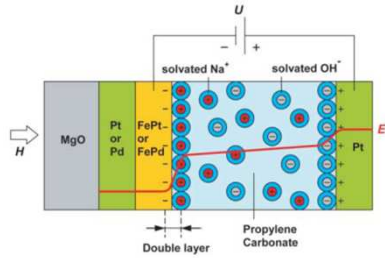


M. Overby *et al.*, Appl. Phys. Lett **92**, 192501 (2008); A. W. Rushforth *et al.*, Phys. Rev. B **78**, 085314 (2008); S. T. B. Goennenwein *et al.*, phys. stat. sol. (RRL) **2**, 96 (2008); C. Bihler *et al.*, Phys. Rev. B **78**, 045203 (2008).

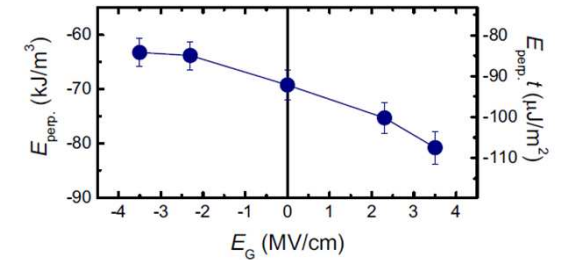
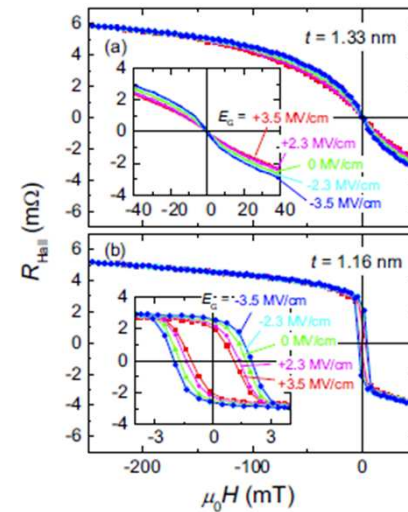
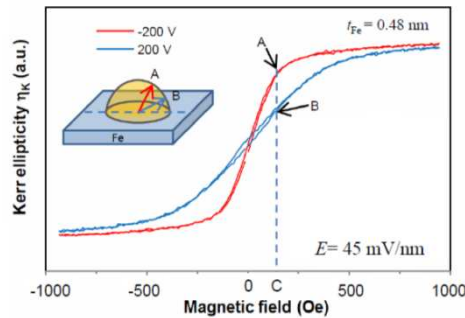
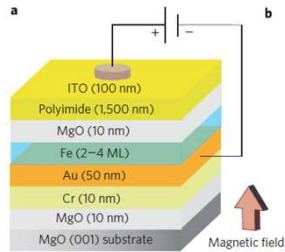
Electric-field control of magnetization direction



Electric-field effects on metals



FePt, FePd: M. Weisheit *et al.*, Science (2007).



Au/ ultrathin Fe: T. Maruyama *et al.*, Nature Nanotechnology (2009).

CoFeB: M. Endo, S. Kanai, S. Ikeda, F. Matsukura, and H. Ohno, *Appl. Phys. Lett.* 2010

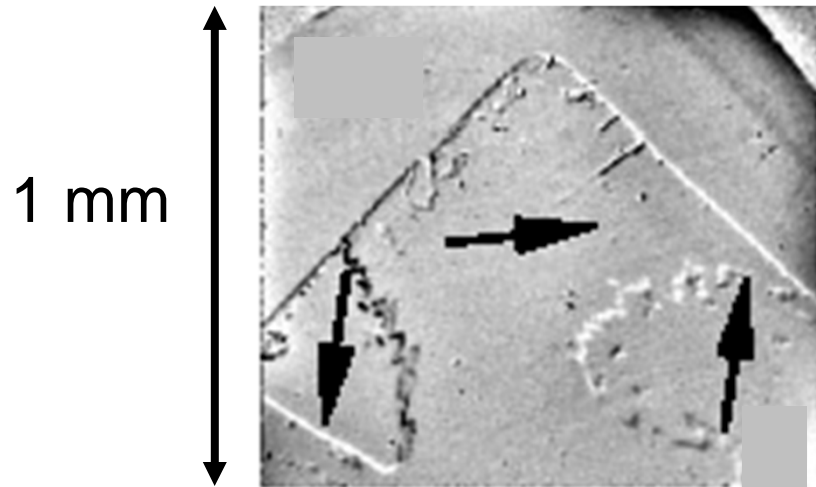
All at room temperature

O-23 Kanai et al.

4. Making “use” of ferromagnetism in semiconductors

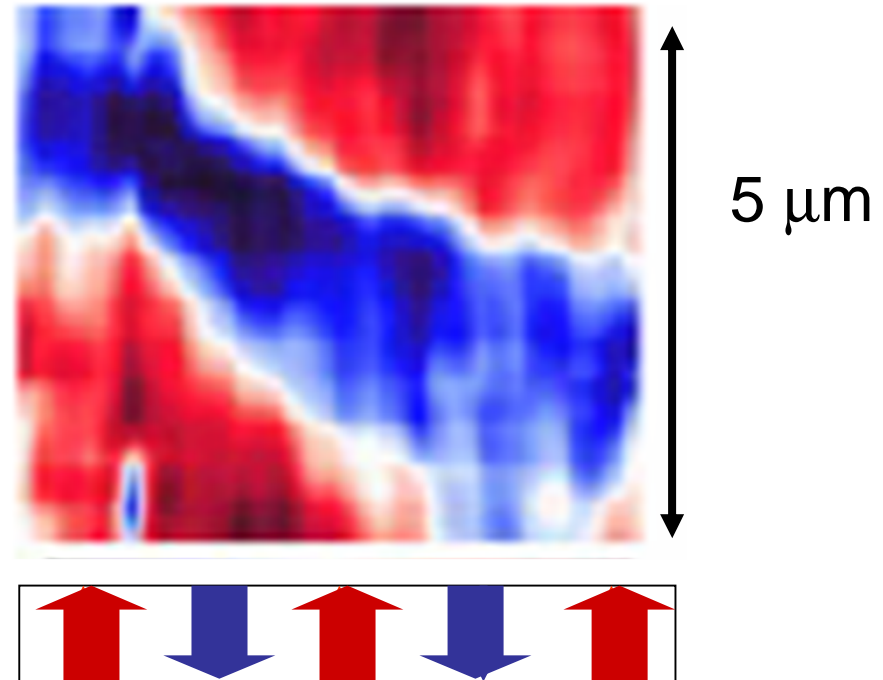
- Electrical control of ferromagnetism
- **Current induced domain wall motion**
- Tunneling with magnetism

Well defined domains: (Ga,Mn)As



Welp et al., PRL 2003

compressive strain
in-plane easy axis
90° domains

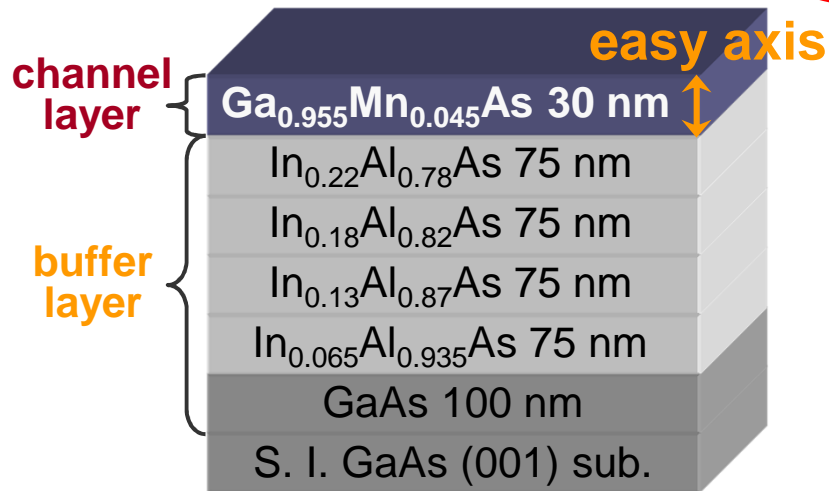


Shono et al., APL 2000

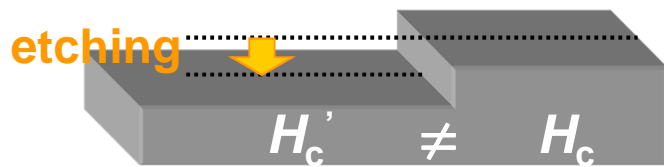
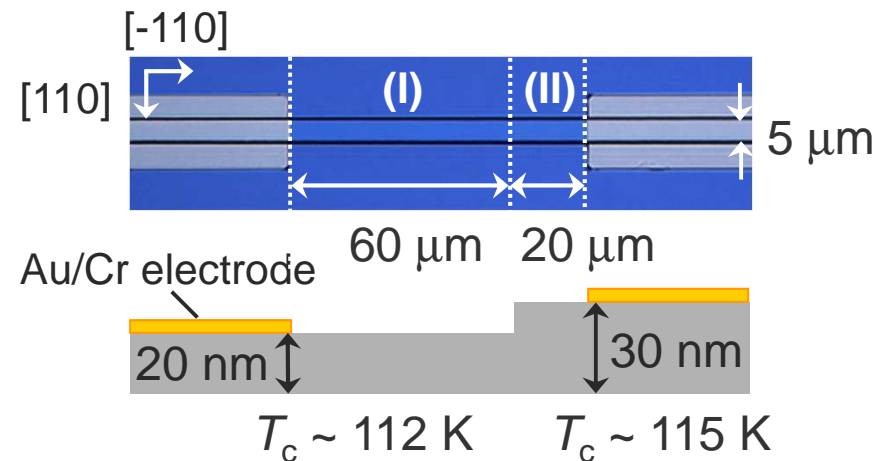
tensile strain
perpendicular easy axis
stripe domains

Current induced domain wall motion

Sample structure



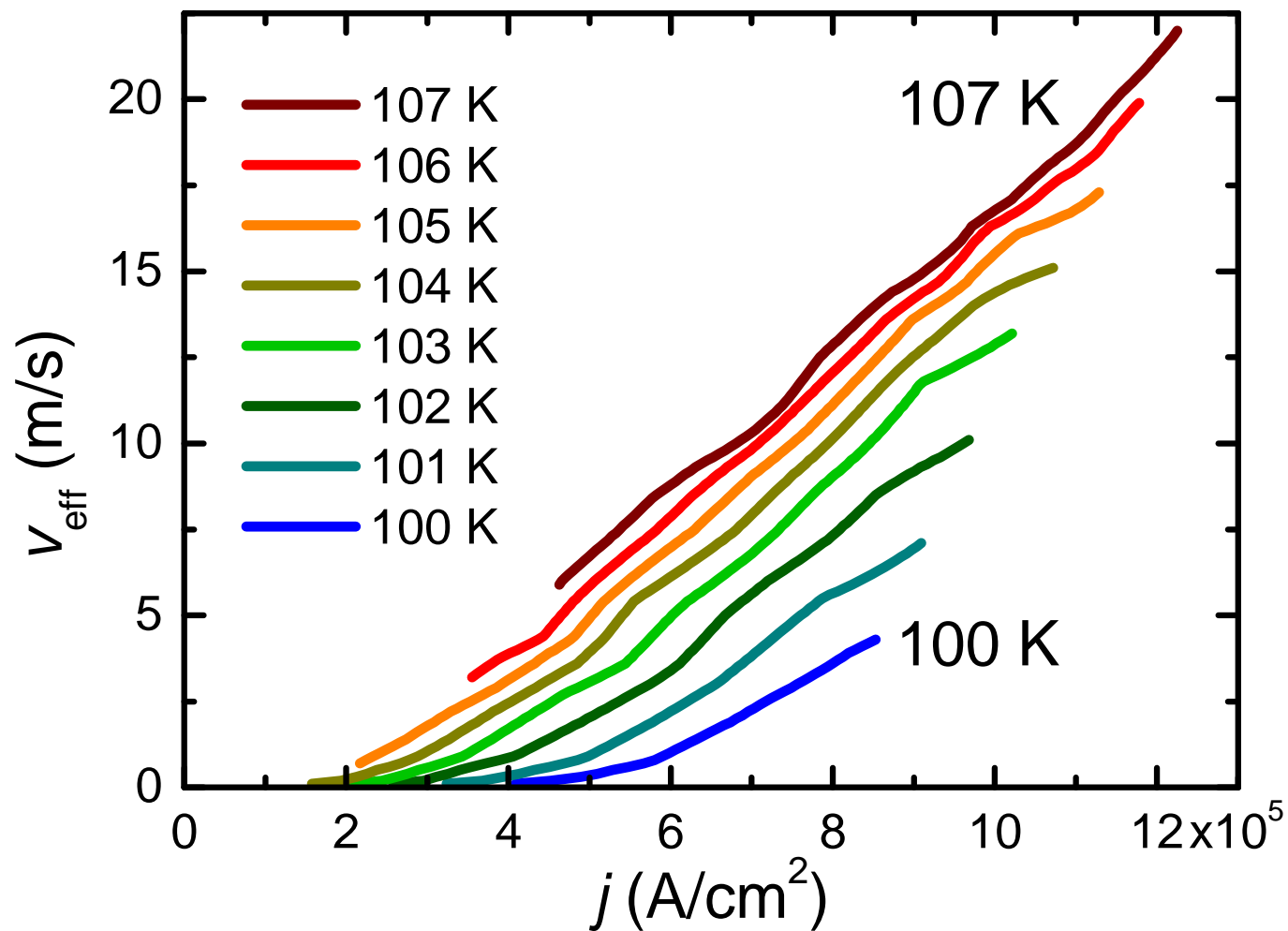
perpendicular easy axis



Patterning of coercive force H_c by etching of (Ga,Mn)As

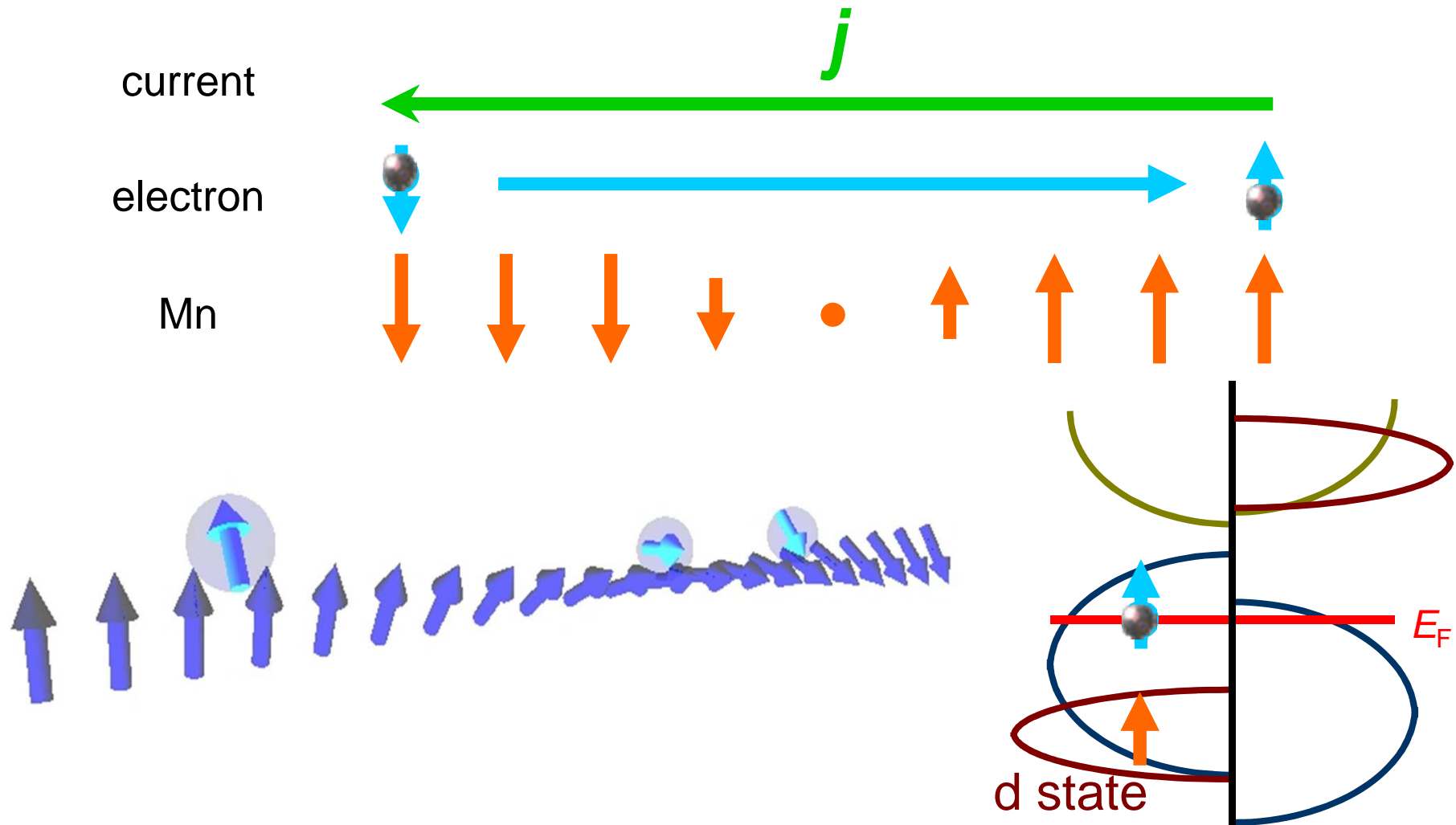
Preparation of domain wall

Current induced domain wall motion



Mechanism

- ◆ Adiabatic spin transfer
(conservation of angular momentum)



Domain wall motion: Theory

- **Square root dependence** (Spin transfer)

G. Tatara and H. Kohno, Phys. Rev. Lett. 92, 086601 (2004).

$$v = A (j^2 - j_C^2)^{1/2}$$

$$A = \frac{P g \mu_B}{2 e M}$$

$$j_C = \frac{2 e K \delta_w}{\pi \hbar P}$$

P : spin polarization

g : g factor of Mn spin

μ_B : Bohr magneton

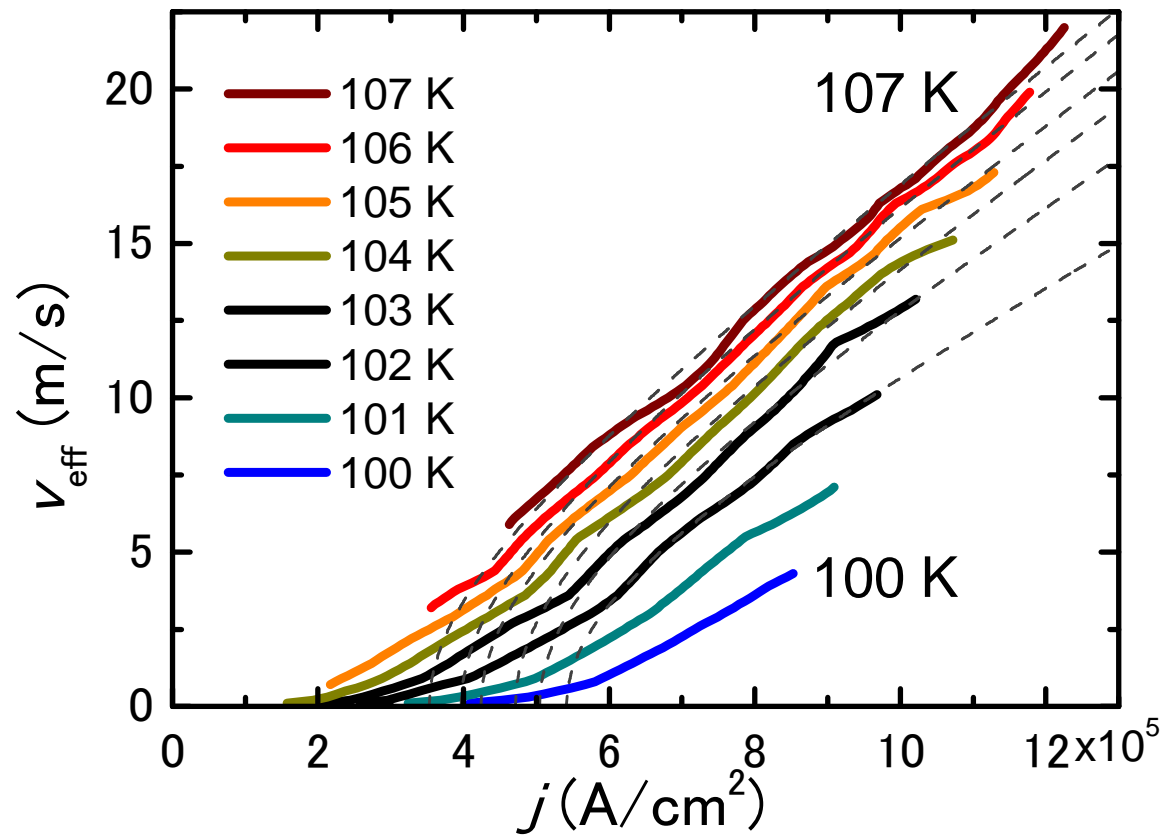
e : charge of electron

M : magnetization

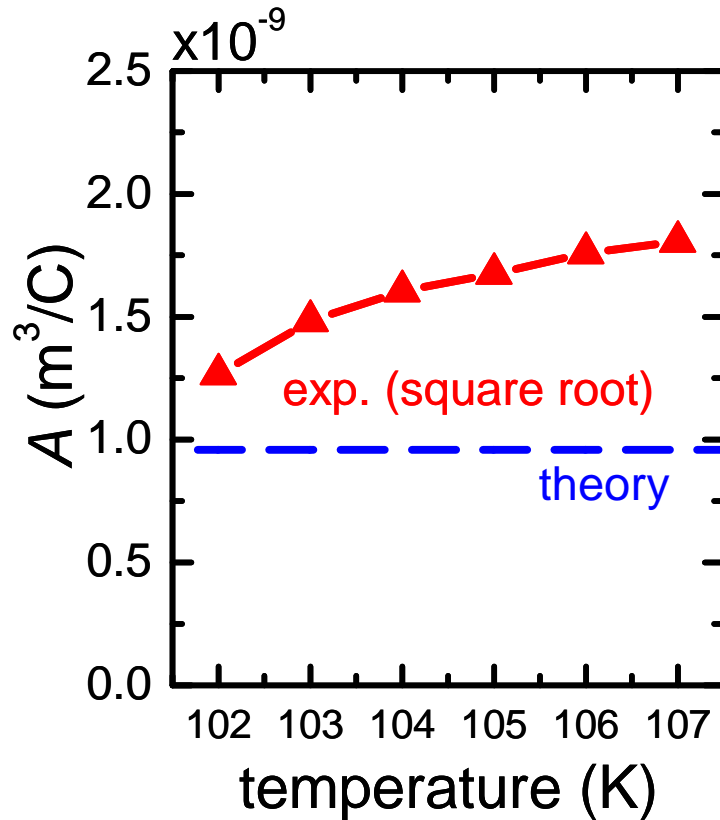
K : transverse anisotropy

δ_w : DW width

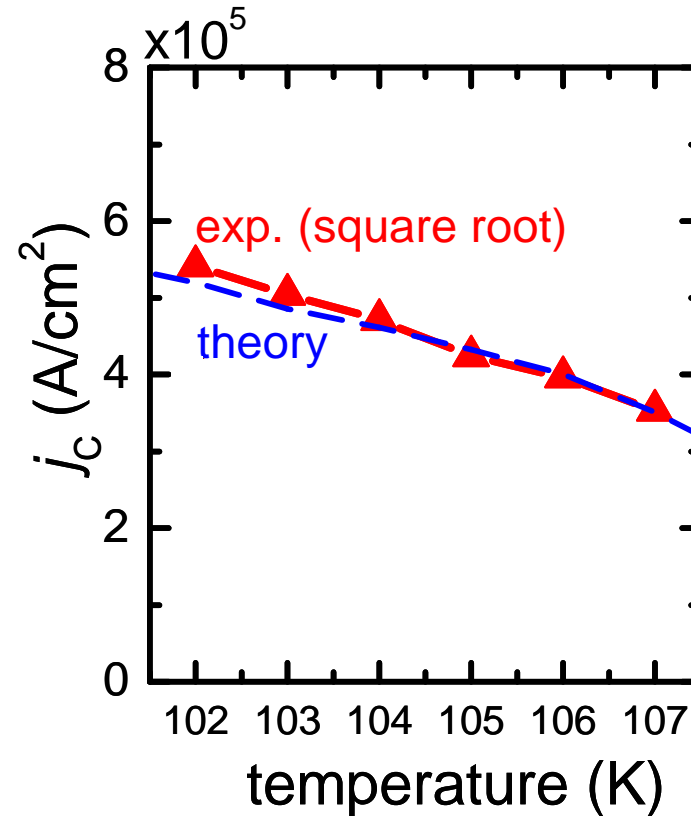
Current induced domain wall motion



Transfer factor and threshold current density



$$A = \frac{P g \mu_B}{2 e M}$$



$$j_c = \frac{2 e K \delta_w}{\pi \hbar P}$$

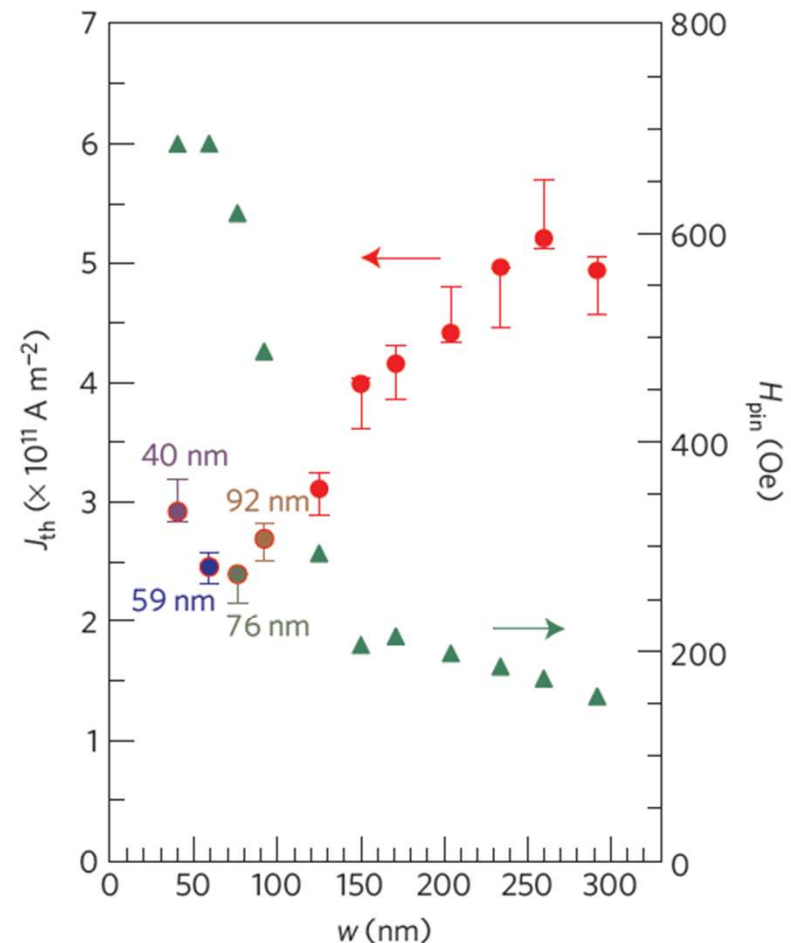
$$j_c = \frac{2eK\delta_w}{\pi\hbar P}$$

	(Ga,Mn)As ($T/T_c \sim 0.9$)	Metal (in plane)	Metal (perpendicular)
K (hard axis anisotropy, J/m ³)	60	4×10^5	10^5
δ_w (domain wall width, nm)	20	100	10
P (spin polarization, %)	20	60	60
j_c (A/m ²)	6×10^9	7×10^{13}	2×10^{12}

Observation of the intrinsic pinning of a magnetic domain wall in a ferromagnetic nanowire

T. Koyama¹, D. Chiba^{1,2}, K. Ueda¹, K. Kondou¹, H. Tanigawa³, S. Fukami³, T. Suzuki³, N. Ohshima³, N. Ishiwata³, Y. Nakatani⁴, K. Kobayashi¹ and T. Ono^{1*}

The spin transfer torque is essential for electrical magnetization switching^{1,2}. When a magnetic domain wall is driven by an electric current through an adiabatic spin torque, the theory predicts a threshold current even for a perfect wire without any extrinsic pinning³. The experimental confirmation of this 'intrinsic pinning', however, has long been missing. Here, we give evidence that this intrinsic pinning determines the threshold, and thus that the adiabatic spin torque dominates the domain wall motion in a perpendicularly magnetized Co/Ni nanowire. The intrinsic nature manifests itself both in the field-independent threshold current and in the presence of its minimum on tuning the wire width. The demonstrated domain wall motion purely due to the adiabatic spin torque will serve to achieve robust operation and low energy consumption in spintronic devices⁵⁻⁸.



4. Making “use” of ferromagnetism in semiconductors

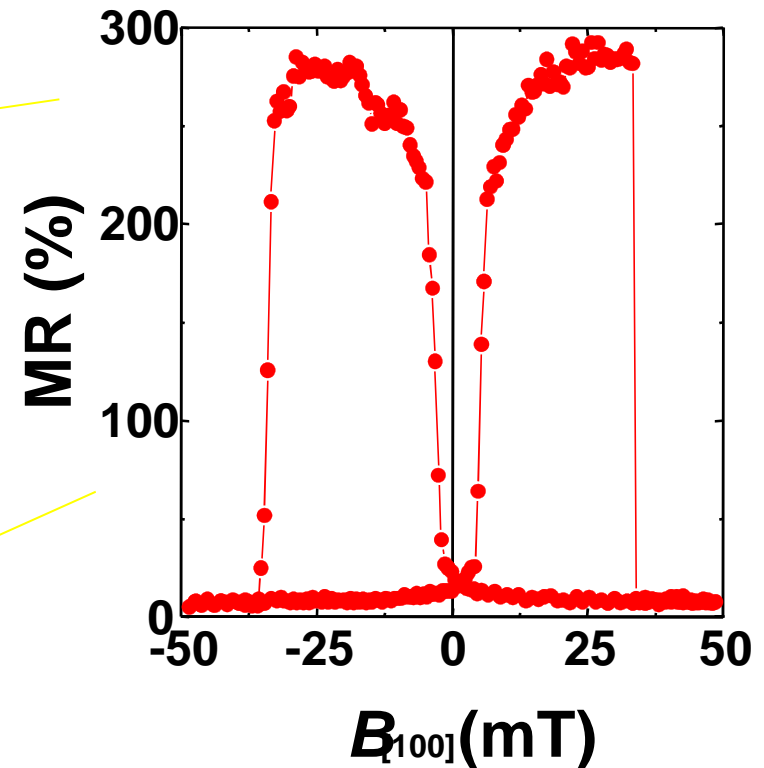
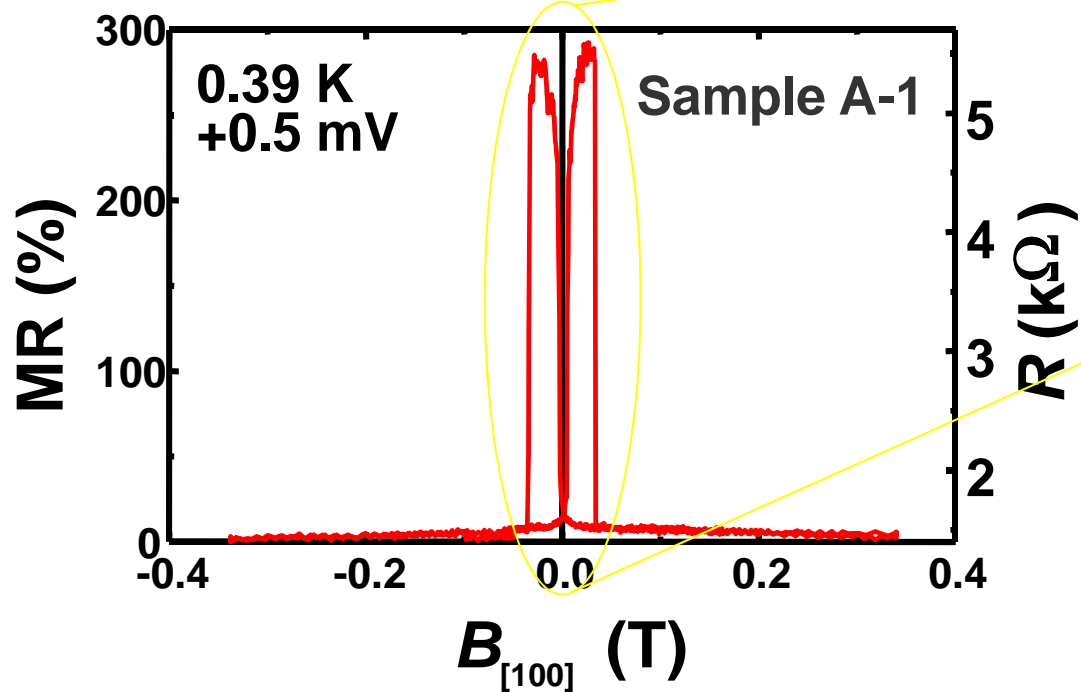
- Electrical control of ferromagnetism
- Current induced domain wall motion
- **Tunneling with magnetism**

Tunnel Magnetoresistance (TMR)

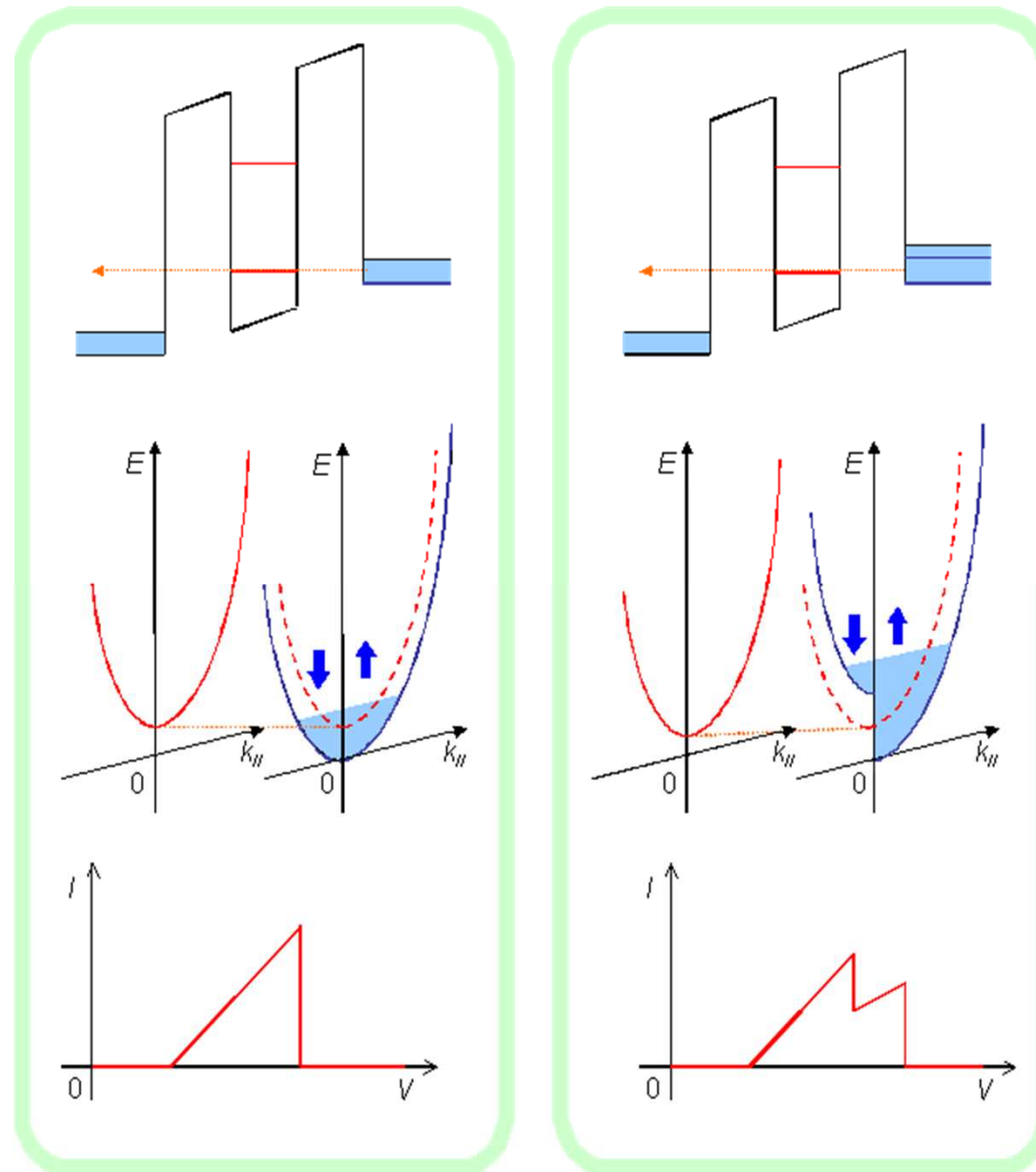
$$TMR = \frac{2P^2}{1 - P^2}$$

20 nm	(Ga _{0.926} Mn _{0.074})As	230-240 °C
6 nm	GaAs	250 °C
20 nm	(Ga _{0.956} Mn _{0.044})As	250 °C
50 nm	GaAs:Be	560 °C
<i>p</i> ⁺ - GaAs (001) sub		

290 %, P = 77 %



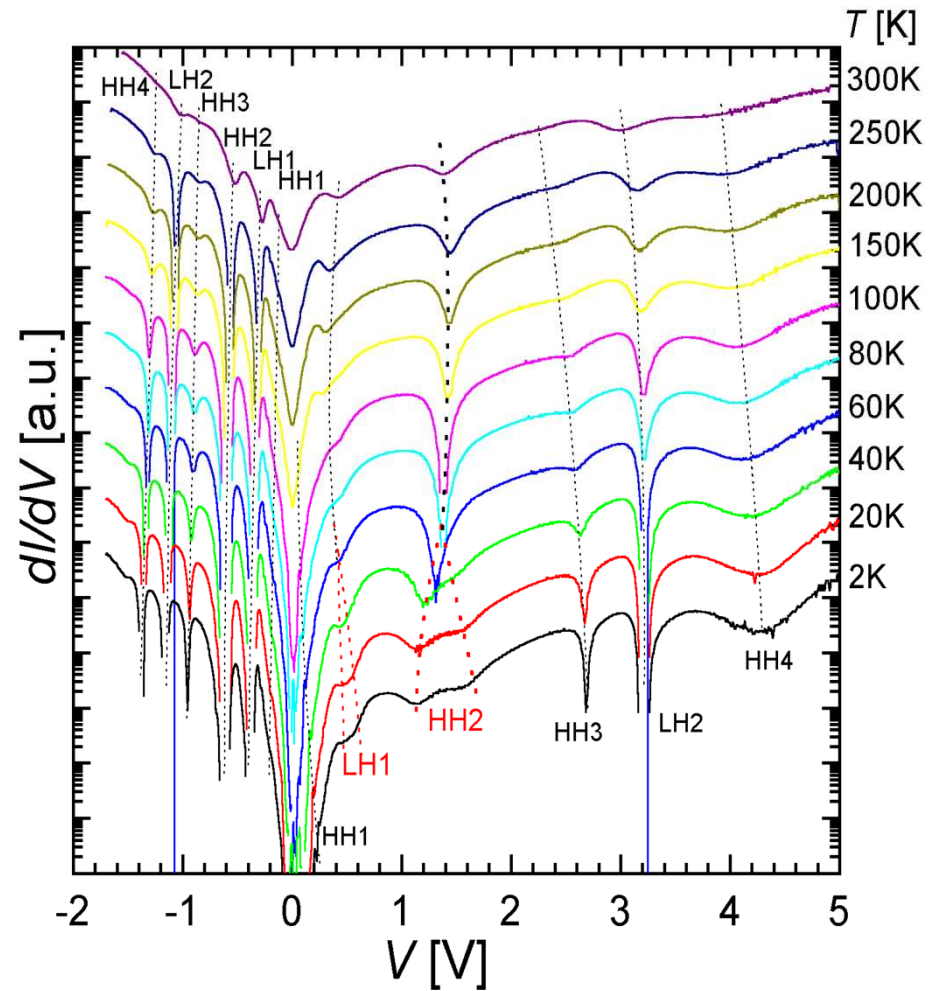
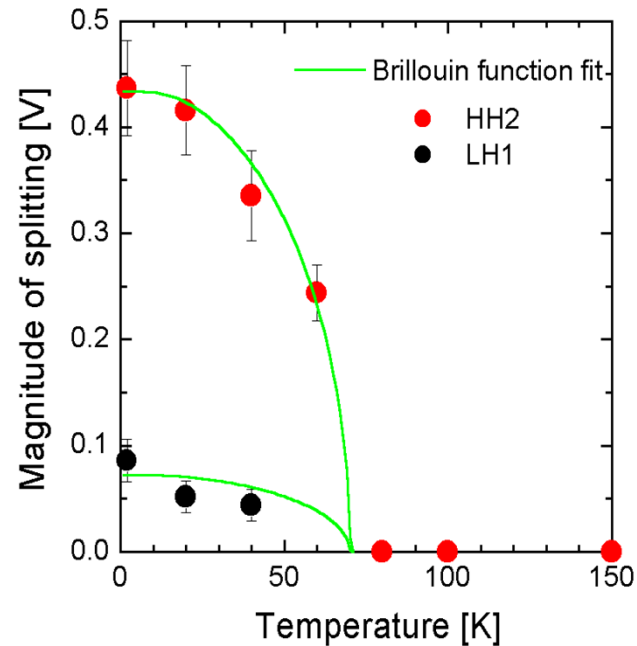
Resonant Tunneling Diode with a Ferromagnetic Emitter



Resonant Tunnel Diode with a Ferromagnetic Emitter

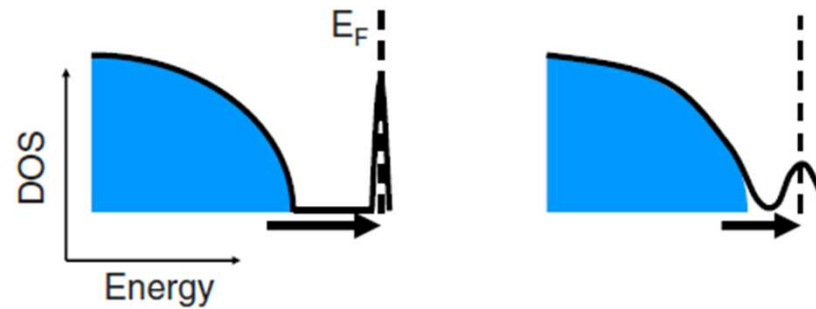
Sample structures

$(\text{Ga}_{0.965}\text{Mn}_{0.035})\text{As}$	200 nm
GaAs	15 nm
AlAs	5 nm
GaAs	d_w nm
AlAs	5 nm
GaAs	5 nm
GaAs:Be ($5 \times 10^{17} \text{cm}^{-3}$)	150 nm
GaAs:Be ($5 \times 10^{18} \text{cm}^{-3}$)	150 nm
p^+ GaAs sub.	

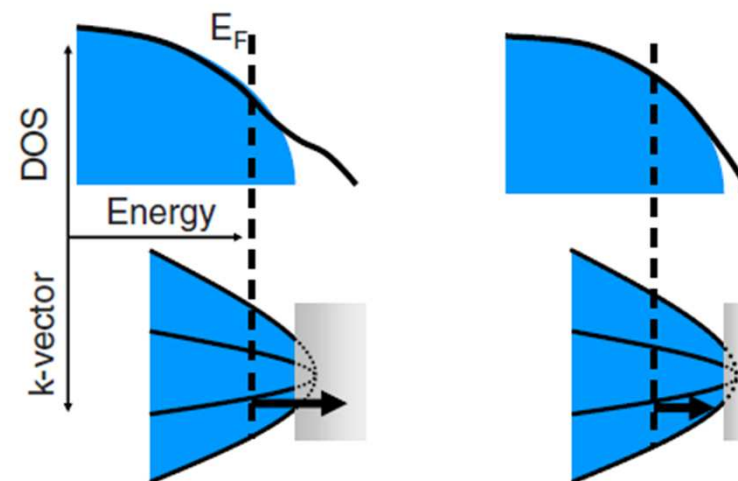


Ultra-high doping of Mn in III-V compounds

Insulating – impurity band detached from valence band



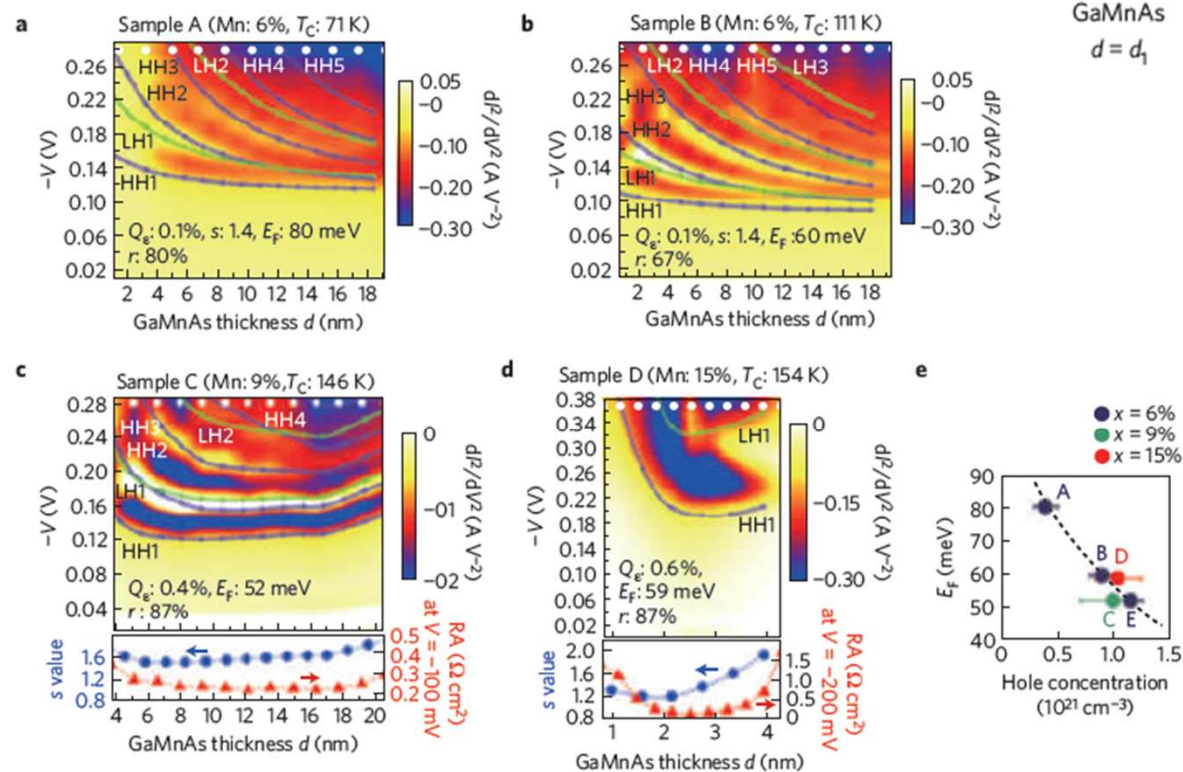
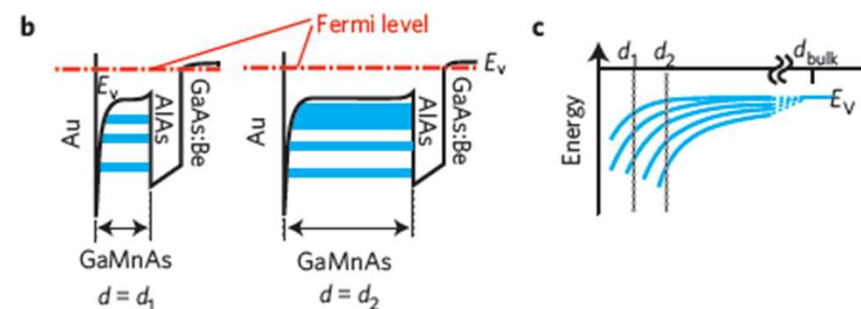
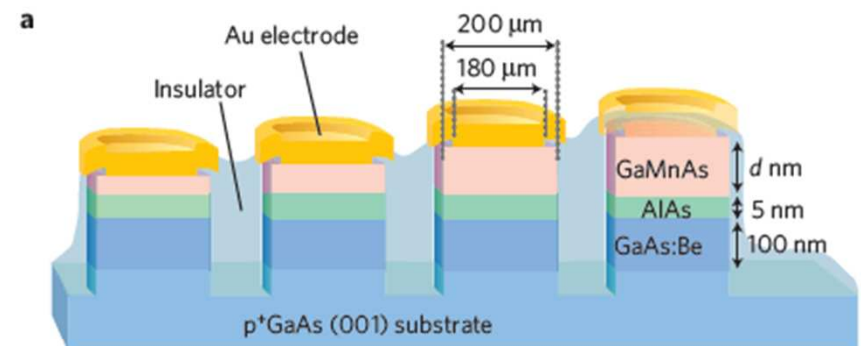
Metallic - merged impurity and valence bands



Nearly non-magnetic valence band of the ferromagnetic semiconductor GaMnAs

Shinobu Ohya*, Kenta Takata and Masaaki Tanaka*

Spintech VI, O-10

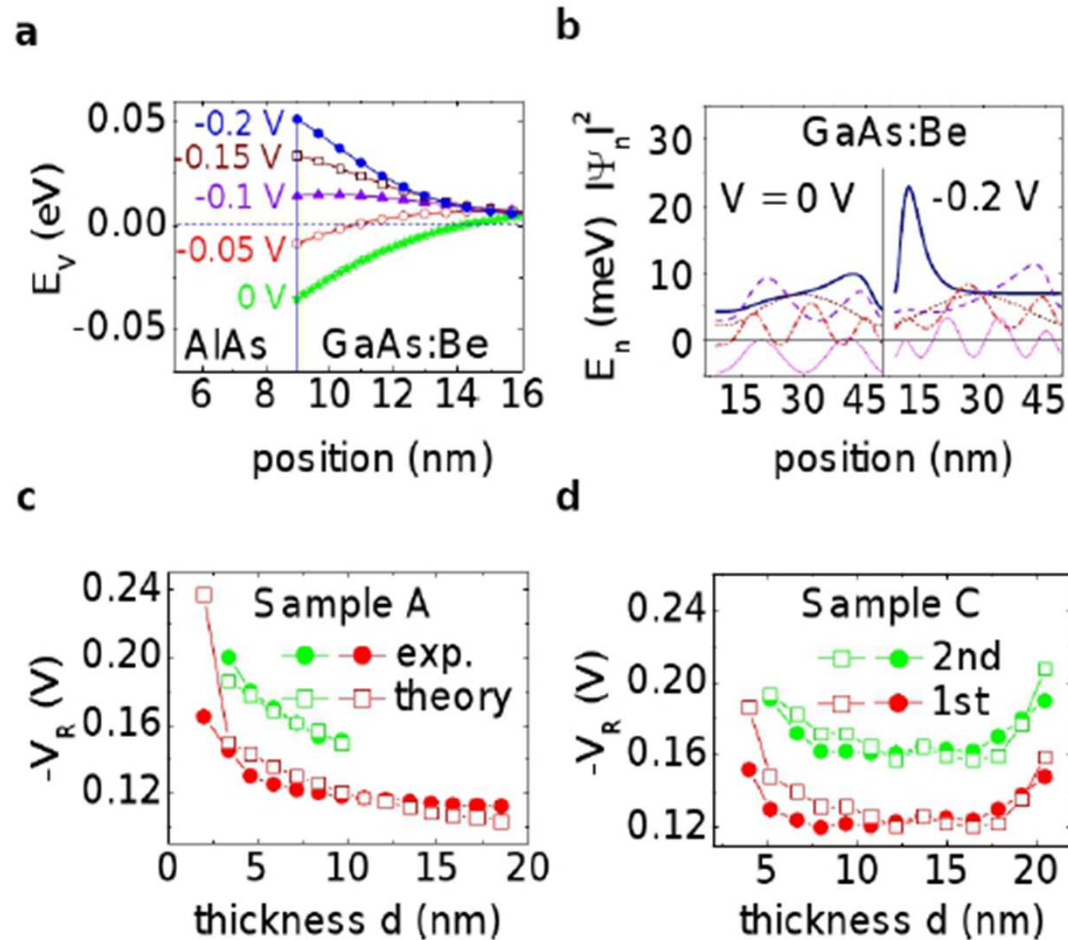


Reconciling results of tunnelling experiments on (Ga,Mn)As

T. Dietl^{1,2} and D. Sztenkiel¹

arXiv 1102.3267v2 (Spintech VI poster FP-42)

(Formation of 2D holes in GaAs:Be explains the resonant tunnel-like feature and the thickness dependence)



Diluted Magnetic Semiconductors

1. What you need to know about nonmagnetic semiconductors
 - Band structure
2. How you make a semiconductor magnetic
 - Doping and *sp-d* exchange
3. The consequences of exchange interaction
 - Spin-split bands and ferromagnetism
4. Making “use” of ferromagnetism in semiconductors
 - Electrical control of ferromagnetism
 - Current induced domain wall motion
 - Tunneling with magnetism